CNRS
Centre National de la Recherche Scientifique

INFN
Instituto Nazionale di Fisica Nucleare

Online h(t) reconstruction for Virgo O3 data: start of O3

D. Estevez, B. Mours, L. Rolland, D.Verkindt

VIR-0652B-19

September 20, 2019

VIRGO * A joint CNRS-INFN Project
Project office: Traversa H di via Macerata - I-56021 S. Stefano a Macerata, Cascina (PI)
Secretariat: Telephone (39) 50 752 521 – Fax (39) 50 752 550 – e-mail virgo@pisa.infn.it

Contents

1 Introduction **3**

2 Main features of the algorithm **4**
2.1 Reconstruction algorithm, main differences since O2 reprocessing 4
2.2 Hrec code version 4
2.2.1 Modifications between v3r03 and v3r09 4
2.3 HRec configuration 5
2.4 Noise subtraction 5
2.4.1 Known issue with noise subtraction during O3a 6
2.5 Contribution of the various signals into h(t) 7
2.6 Measured optical gains and finesses 7

3 Produced data **12**
3.1 Data quality flags and associated channels 12
3.2 Generated $h(t)$ channels 13
3.3 Output files 14

4 Reconstruction validations and uncertainty estimation **16**
4.1 $h(t)$ sign definition and validation 16
4.2 Validation of $h(t)$ with hardware injections 20
4.2.1 Validation of $h(t)$ with hardware injections using photon calibrators . . . 20
4.2.2 Validation of $h(t)$ with hardware injections using electromagnetic actuators 24
4.2.3 Remarks on $h(t)$ validation with weekly hardware injections 24
4.2.4 Monitoring of $h(t)$ stability with permanent hardware injections 28
4.2.5 Estimation of $h(t)$ uncertainties 31

5 Plans for reprocessing and HRec improvements **32**

A Validation of $h(t)$ with hardware injections: stability **36**

B HRec configuration files used online **41**
B.1 Main file: HRec.cfg 41
B.2 Description of main input channels: HRec_MainChannels_FromPCal.cfg 43
B.3 Description of hardware injection channels: HRec_CalChannels_fromPCal.cfg . 44
B.4 Description of noise subtraction channels: HRec_NoiseChannels.cfg 45

C Other online HRec configurations **45**

1 Introduction

The O3 LIGO-Virgo run started on April 1st, 2019, 15h UTC. This note describes the online reconstruction of the Advanced Virgo data collected at the start of O3 run. The software version and process configuration described in this note are still running at the time of writing this note (June 2019). Updates will probably happen before the end of O3 following improvements in the calibration models or improvements in the h(t) reconstruction software.

Section 2 gives an update of the main differences of the code with respect to the version used for the latest O2 reprocessing. The HRec configuration and subtracted noise are also given, as well as some standard checks. Section 3 describes the produced channels and flags and how they are stored. Finally, the $h(t)$ sign validation and estimation of the systematic uncertainties are described in section 4. Some more information about HRec stability, the full configuration file, and a rough description of the other HRec configurations running online for other purpose are given in appendix.

The data used for the online reconstruction is from March 16th to 29th, 2019 (GPS period 1236750000 to 1237900000). The models have been derived from the photon calibration technic described in [1].

2 Main features of the algorithm

2.1 Reconstruction algorithm, main differences since O2 reprocessing

The algorithm used for the $h(t)$ reconstruction is the same as the one used for initial Virgo and for O2 run. It has been documented in thesis, Virgo notes [2, 3] and publications [4].

The logic of the code is to take the dark fringe signal, to remove the contributions of the control signals by subtracting the corrections applied to the various mirrors and correct for the optical transfer function. This procedure does not correct the effect of the control loops by applying a transfer function, but by subtracting their contributions. Therefore, some of the residual control signals, like the calibration lines, are removed/reduced thanks to this technic.

The optical model used for O3, for a simple cavity, is a 1st order pole depending on the optical gain and cavity finesse. The optical gain and cavity finesse are monitored online from the calibration lines and their small variations are taken into account in the reconstruction. A similar optical model is used for the PR mirror.

In addition, noise subtraction had been added for O2 $h(t)$ reprocessing and the same technic is still being used for O3 online reconstruction: auxiliary monitoring signals are used as noise witness and subtracted from $h(t)$ after applying a transfer function measured on the data and updated every 500 s.

The reconstruction is computed in the frequency domain, using chunks of 8 seconds of data with an overlap of 50%. It reduced the reconstruction latency from 20 to 8 s compared to O2 when chunks of 20 s were used.

2.2 Hrec code version

The code used for $h(t)$ reconstruction is the Hrec.exe application from the Hrec package available from the Virgo SVN repository. The used version of June 2019 is v3r09, installed in /virgoApp directory.

2.2.1 Modifications between v3r03 and v3r09

Between the version v3r03 used for the second reprocessing of O2 data and the version v3r09 running for O3 online reconstruction, the main code modifications are:

- update the Fd library version to the one used for the O3 run: v8r30. It includes in particular the latest gating tools.
- add the key GET_OGAIN_FREQ_BCKGRND to ...
- add the key SHAPING_FILTER to ...

- apply the finesse limits on the median value instead of the single computed values
- add the option to have different low frequency cut-off for different output channels: useful to provide a $h(t)$ channel sampled at 200 Hz and a cut-off at 2 Hz.
- add the option to produce intermediate output channels: useful to output channels with or without the different noise subtraction applied.
- add the key OUTPUT_PREFIX: useful to have different hrec applications running with different parameters and producing output channels with different prefixes.

2.3 HRec configuration

The HRec.cfg configuration file running online at the start of O3 is reported in appendix B. It is read online from /virgoData/VirgoOnline directory.

The actuator models used in the configuration are the models derived end of March 2019 using the pre-O3 calibration data.

The models for NE and WE actuators are based on the measurements made with the photon calibrators. The models for the BS and PR actuators are the one measured with the free swinging Michelson technic, but renormalized by the difference between photon calibration and free Michelson calibration. The two actuator calibration results and their comparison are described in three notes [1, 5, 6].

2.4 Noise subtraction

The noise subtraction technic is the same as the one developed and used for the second reprocessing of O2 data (V1O2Repro2A). The residual transfer function between a witness channel and $h(t)$ is computed periodically (in practice every 500 s). The computation is done only if the BNS range is above a given value, set to 18 Mpc. and if the calibration line signal-to-noise ratio is large enough. Then this transfer function is applied to the next 500 s chunk of data for the frequency bins that have coherence above a given value: the frequency resolution is 0.625 Hz and the coherence threshold is 4%.

In the case of multiple witness channels, this technic works only if the witness channels do not witness the same noise. If they are partially correlated and show some coherence, the noise will be subtracted more than once, which implies that it will be re-added in $h(t)$ instead of being subtracted.

Different sources of noise were identified in the weeks before the start of O3 and have been subtracted:

- V1:SPRB_B4_56MHz_Q: witness of MICH control noise, in the range 8 to 90 Hz. This also removes some residual noisecoming from the innaccuracy of the model for the optical response to PR mirror motion.
- V1:SIB2_B2_8MHz_I: witness of frequency noise (PRCL noise), in the range[1] 90 to 3500 Hz.
- V1:SDB2_B1s1_PD1_Blended: witness of the 56 MHz relative intensity noise, in the range 40 to 1000 Hz.
- V1:SNEB_B7_DC: witness of the scattered light on NE end bench, in the range 10 to 70 Hz.
- V1:SWEB_B8_DC: witness of the scattered light on WE end bench, in the range 10 to 70 Hz.

As the first two witness channels are coherent in part of the spectrum, the frequency range where the estimated noise is subtracted has been separated into two distinct ranges.

The scattered light subtraction only removes a few peaks in the spectrum.

2.4.1 Known issue with noise subtraction during O3a

It has been found (see logbook entry 45637) that the BNS range is sometimes going down by few Mpc for periods of 500 s started at a GPS time multiple of 500. This is related to the noise subtraction whose transfer functions are updated every 500 s. In general, a drop in the horizon is seen in the previous 500 s segment. The conclusion is that glitches are sometimes polluting the estimation of the transfer function which is applied for noise subtraction in the next segment.

In August, tests have been done to increase the BNS range threshold to allow for transfer function computation: increasing the threshold slightly reduces the number of such noisy segments, but too high treshold prevents the noise subtraction to work once the BNS range stays below the treshold.

As another test, the transfer function was computed using median instead of average. In this configuration, there was no more noisy segments (among a handfull of them that were reprocessed), but the BNS range was lower by 1 or 2 Mpc everywhere.

Other investigations are on-going to improve this behavior and be insensitive to glitches in the transfer function computations. In addition, a method using a covariance matrix between the witness channels will be developped in order to remove only once a noise contribution that may be seen in more than one witness channel.

[1] From August 1st 2019, the limit frequency between MICH noise and frequency noise was moved from 90 Hz to 150 Hz, see logbook entry 46518 and comments.

2.5 Contribution of the various signals into h(t)

The typical contributions of the control signals used to build $h(t)$ are shown in figure 1(a) and 1(b). and the contributions from the subtracted noise are shown in figure 2(a).

We can observe that:

- the mirror controls are almost negligible in $h(t)$ above about 500 Hz.
- the frequency noise contribution is in general low, except for some bumps, but sometimes increases and contribute at high frequency.
- the PRCL control noise is coupled to B1 signal up to about 100 Hz and its subtraction is important. This subtraction also correct $h(t)$ for the innaccurate optical model used for the interferometer response to PR mirror motion.
- the other subtracted noises have negligible contribution in general.

2.6 Measured optical gains and finesses

The typical time series and distributions of the optical gains and finesses are shown in figures 3 and 4, over a lock segment of 14 hours.

The finesse value is stable and the fluctuations are dominated by the statistical fluctuations lower than 1% coming from the signal-to-noise ratio (of about 100) of the permanent lines.

In addition, the optical gain values show a slow variation coming from the changing detector working point (alignment, ...). These variations are at the level of 2% for NE, WE and BS.

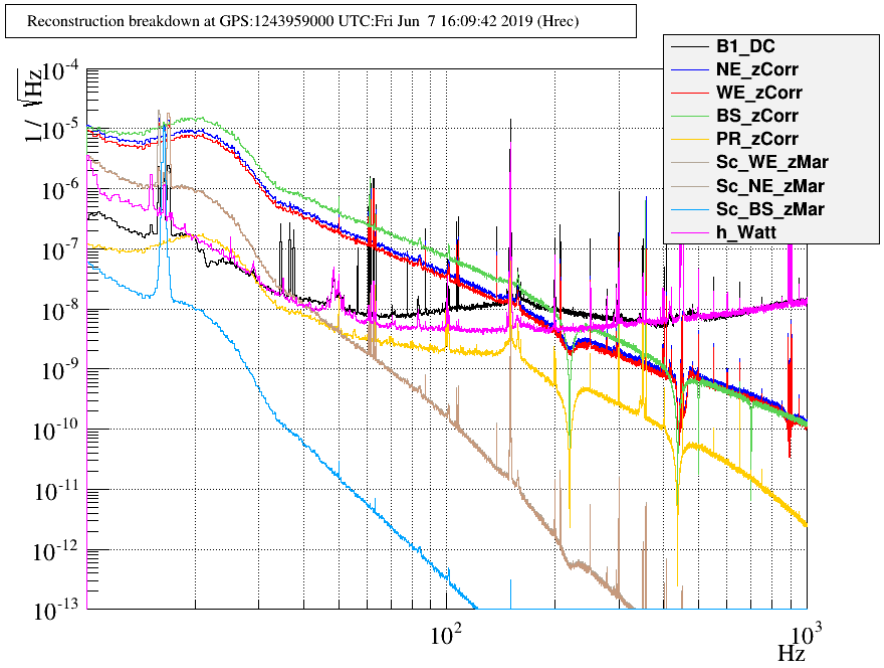

(a) Control signals: raw spectrum

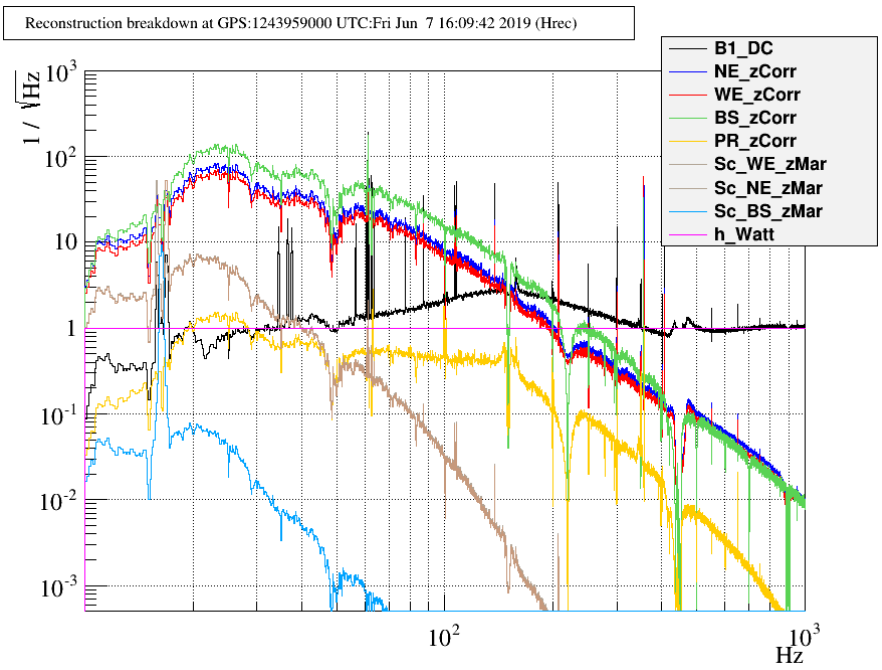

(b) Control signals: normalized spectrum

Figure 1: Typical spectrum of the control signals involved in the reconstruction (GPS 1243959000, on June 7th 2019). Raw spectrum (top) and normalized to the $h(t)$ spectrum (bottom) to see their relative contributions.

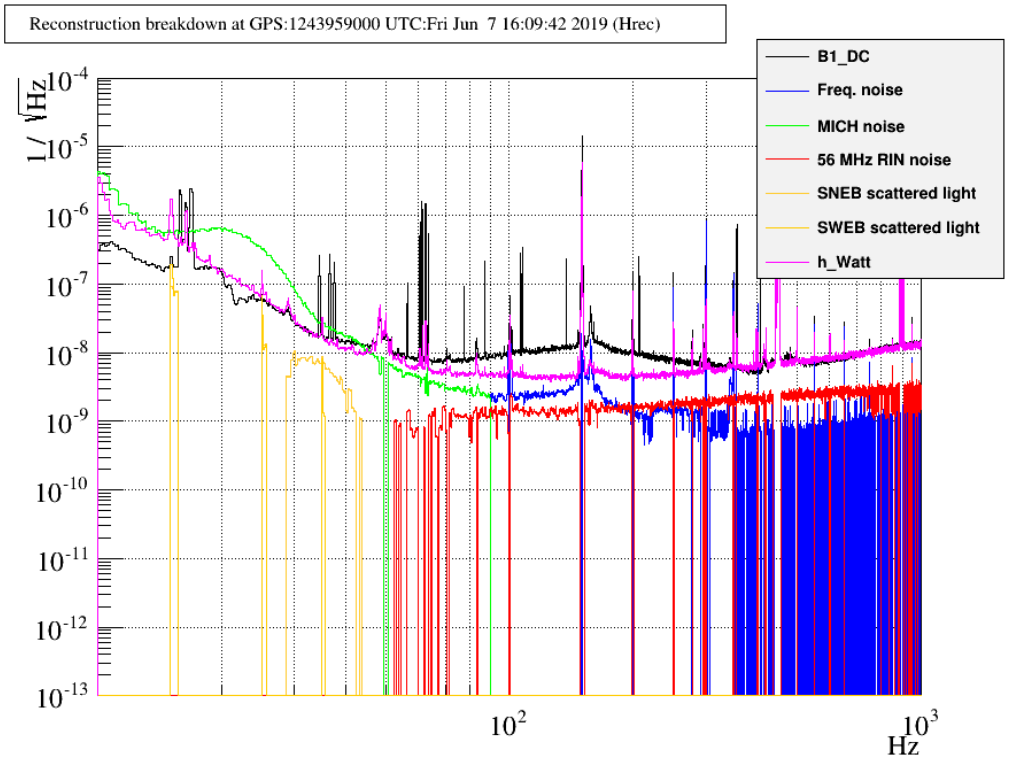

(a) Noise signals: raw spectrum

Figure 2: Typical spectrum of the noise witness signals involved in the reconstruction (GPS 1243959000, on June 7th 2019). Raw spectrum.

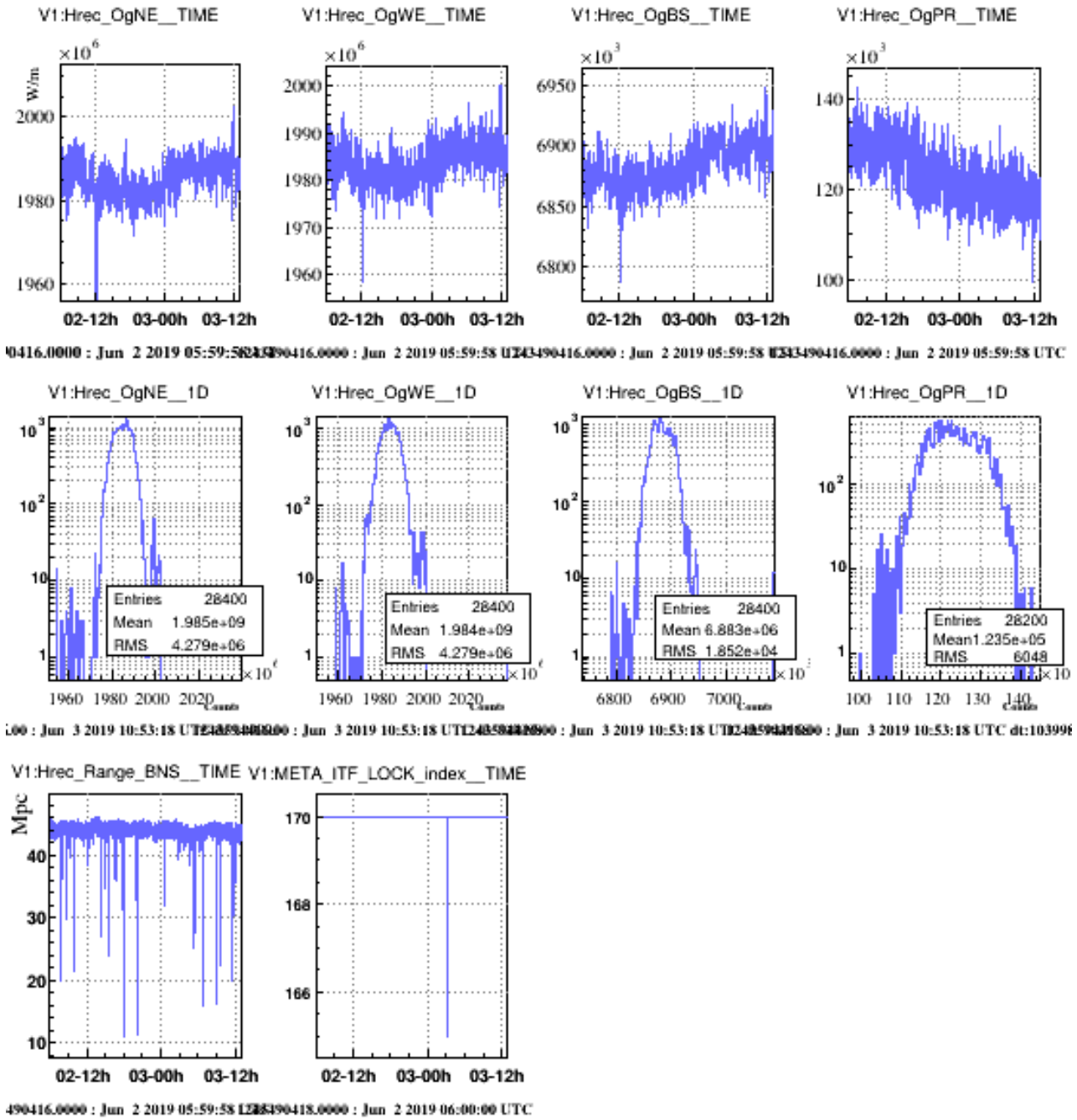

Figure 3: Typical fluctuations of the optical gains for NE, WE, BS and PR. First line: time series of optical gains of NE, WE, BS and PR. Second line: distributions of the NE, WE, BS and PR optical gains. Third line: computed range and lock state in the same time window.

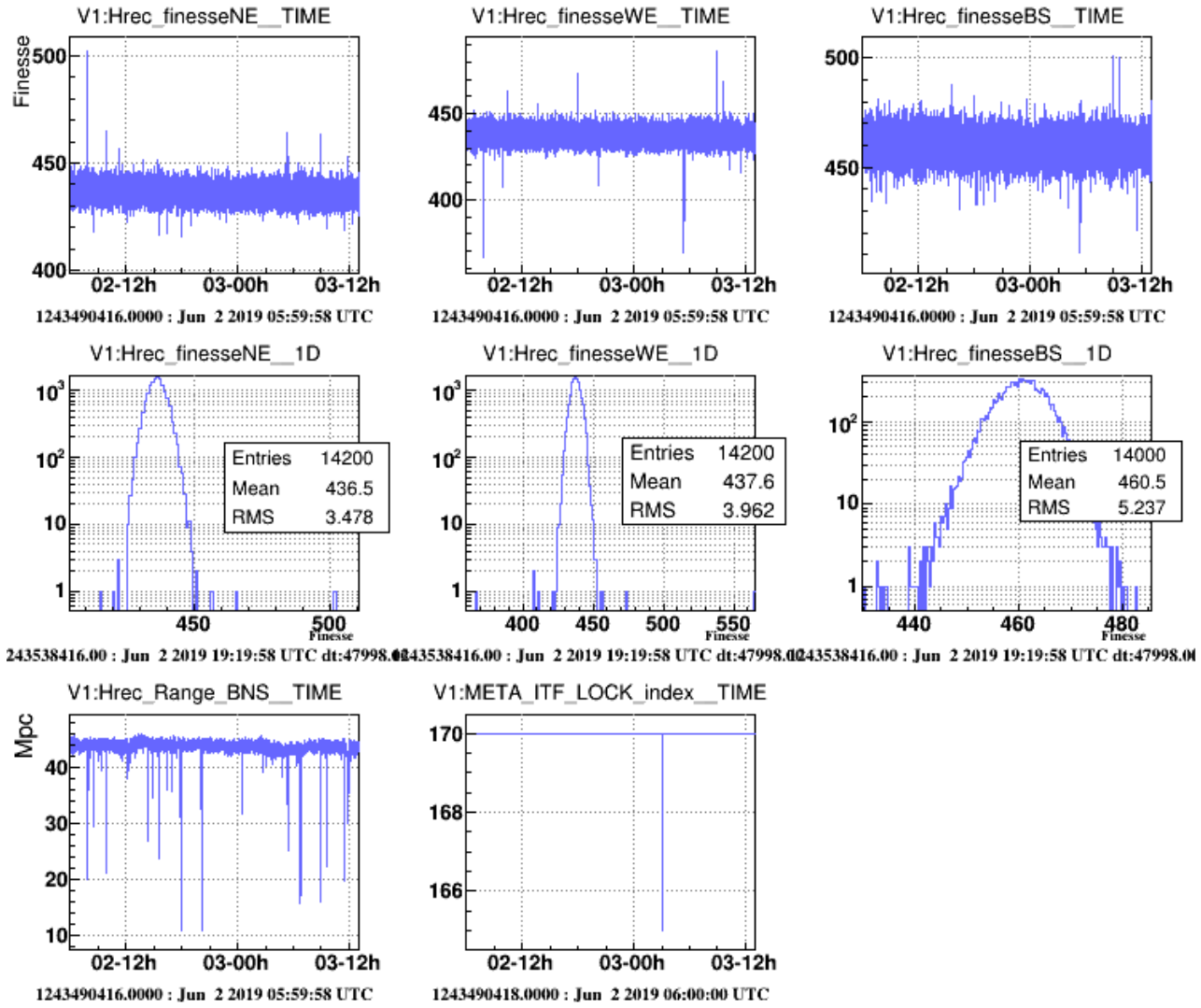

Figure 4: Typical fluctuations of the finesses for NE, WE, BS. First line: time series of finesses NE, WE, BS. Second line: distributions of the NE, WE, BS finesses. Third line: computed range and lock state in the same time window.

3 Produced data

3.1 Data quality flags and associated channels

The $h(t)$ quality is evaluated every 4 seconds. The conditions to get a good quality are:

- The interferometer is locked (V1:META_ITF_LOCK_index >= 159). During O3, it corresponds to LOW_NOISE_3 or LOW_NOISE_3_SQZ states.
- All the channels needed for the frequency-domain filtering are available for the current, previous and following 8 second chunks of data,
- The SNR of the NE, WE, BS calibration lines is above 10 (was 3 for O2?).

The results of these tests are recorded in the following ADC channels sampled at 0.25 Hz::

- "V1:Hrec_Flag_Quality" for the overall quality (1 means OK)
- "V1:Hrec_Flag_Frame" if the previous/following frames are present (1 means OK)
- "V1:Hrec_Flag_Channel" if all the needed channels are available (1 means OK)
- "V1:Hrec_Flag_SNR" if the SNR test is OK (1 means OK).

The summary of the data quality information can be found in the state vector: V1:Hrec_STATE_VECTOR.

The bit follows the same definition as the V1:DQ_ANALYSIS_STATE_VECTOR:

- 0: $h(t)$ was successfully computed
- 1: science mode button is pushed
- 2: observation ready
- 3: $h(t)$ was produced by the calibration pipeline
- 4: calibration filters settled in
- 5: No stochastic HW injections
- 6: No CBC HW injection
- 7: No burst HW injection

- 8: No HW injections for detector characterization
- 9: No continuous wave HW injection
- 10: good data quality (CAT1 type)
- 11: interferometer is locked

Bits 0, 3, 4 and 10 are set when the reconstruction is ok (V1:Hrec_Flag_quality = 1). Data can be analyzed when all the bit are at +1, that means V1:Hrec_STATE_VECTOR = 4095 (or 0xFFF).

3.2 Generated $h(t)$ channels

Three $h(t)$ channels are produced online for data analysis use. They are produced after subtraction of different noise and after subtraction of hardware injections:

- V1:Hrec_hoft_20000Hz: main output channel sampled at 20000 Hz.
- V1:Hrec_hoft_16384Hz: main output channel sampled at 16384 Hz.
- V1:Hrec_hoft_16384Hz_Gated: main output channel sampled at 16384 Hz, but with gating applied around big drops in the range.

In addition, some intermediate channels are produced to monitor the noise subtraction:

- V1:Hrec_hoft_raw_20000Hz: channel computed with the minimal needs for $h(t)$, after controls subtraction, but before any additional subtraction of other noise.
- V1:Hrec_hoft_clean_B4_20000Hz: after subtraction of V1:SPRB_B4_56MHz_Q.
- V1:Hrec_hoft_clean_B4_B2_20000Hz after subtraction of V1:SIB2_B2_8MHz_I.
- V1:Hrec_hoft_clean_20000Hz after subtraction of all the other noise, but before the subtraction of the hardware injections (via electromagnetic actuators and photon calibrators).

3.3 Output files

A sketch of the integration of HRec into the data acquisition pipeline and of the online $h(t)$ distribution is shown in figure 5.

As an online process, all the channels described above are stored in the raw data stream circular buffer of about 6 month depth (pointed by /virgoData/ffl/raw.ffl).

In addition, the $h(t)$ channel produced at 16384 Hz is stored in circular buffers in Cascina:

- /data/online/hrec/V1Online/V-V1Online*.gwf is a backup stored for about one month.
- /data/prod/hrec/V1Online/V-V1Online*.gwf keeps that data for about three months. It is pointed by /virgoData/ffl/V1Online.ffl.
- the files from /data/prod/hrec/V1Online/ are moved manually to /virgoData/prod/hrec/O3a/V1Online/ to store all the O3 data for longer term at Cascina. However, this data is supposed to be deleted when O3 is over and the calibration/reconstruction studied completed, hence probably at the beginning of O4.

The files written in /data/online/hrec/V1Online/ are distributed via LDR to the Computing Centers for permanent storage: CCIN2P3, CNAF and CIT.

The Virgo $h(t)$ channel produced at 16384 Hz and associated state vector are sent online to Caltech, using Cm, for online data analysis (via the process V1Cas2CIT1s).

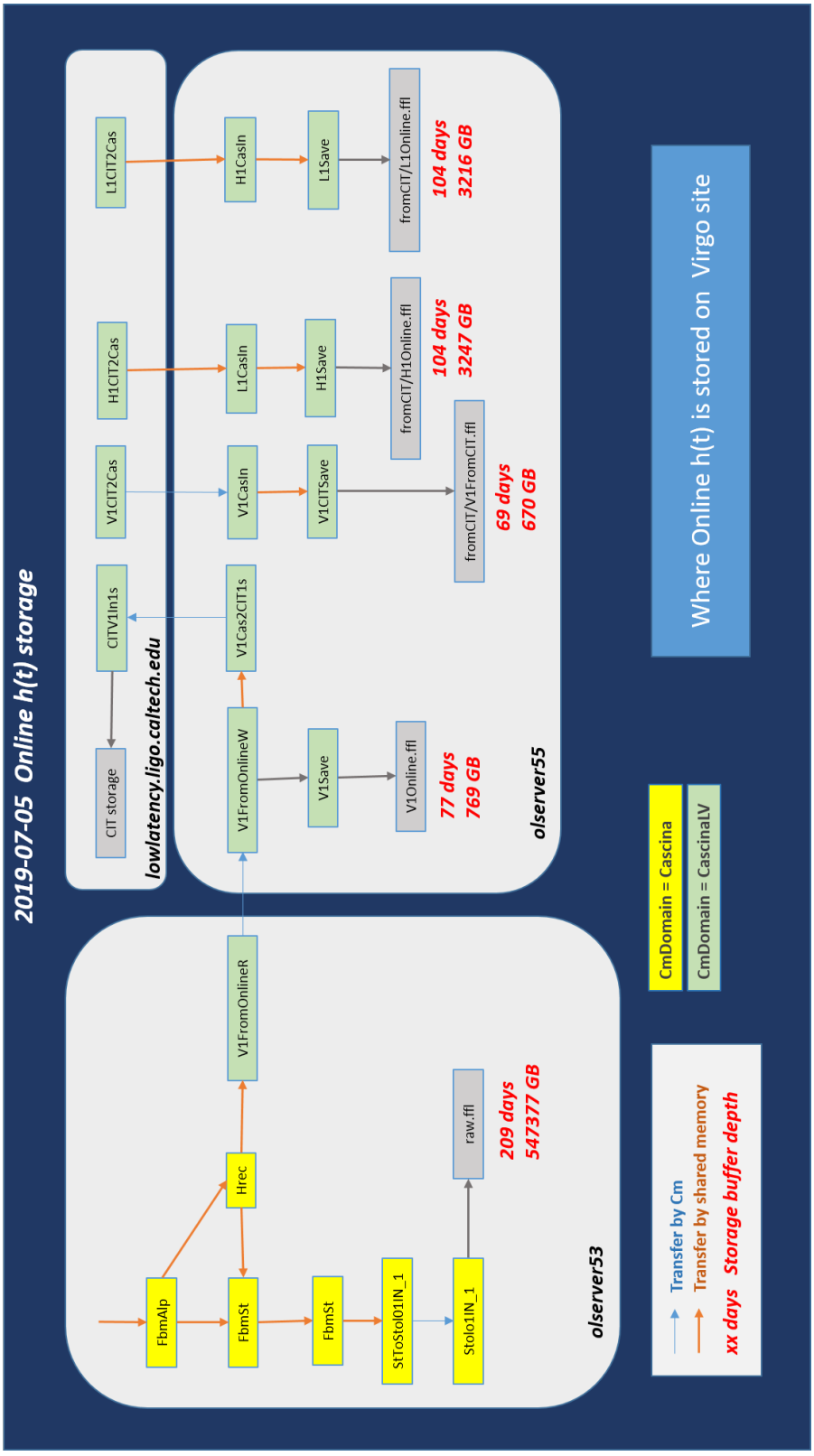

Figure 5: Sketch of the data acquisition pipeline including HRec process and of the HRec output processing towards storage and online distribution.

4 Reconstruction validations and uncertainty estimation

4.1 $h(t)$ sign definition and validation

For Virgo, the $h(t)$ sign is defined as $h(t) = \frac{\delta L_{North} - \delta L_{West}}{L_0}$ (see note [7]). As usual, the sign of $h(t)$ is validated using the photon calibrator (PCal) injections. In addition, during O3, permanent calibration lines sent by a PCal are used to monitor the sign continuously.
.

Since the WE PCal is pushing on WE mirror from inside the Fabry-Perot cavity and at frequencies larger than the pendulum resonance frequency (~ 0.6 Hz), there is phase opposition between the PCal laser power and the cavity length: the West cavity length increases when the PCal laser power decreases (and vice versa). From the $h(t)$ definition, $h(t)$ also decreases: it means that $h(t)$ must be in phase with the PCal laser power. The PCal calibration lines being subtracted in the final $h(t)$ channel output, the validation must be done in the intermediate channel before hardware injection subtraction. Then we check that the $h(t)$ intermediate and final channels are in phase.

The figure 6 (left column) confirms that it is indeed the case looking at the transfer function from the PCal laser power to $h(t)$, and validates that the Pcal laser power channel is positive (i.e. there is no sign flip in the sensing of the PCal laser power). In addition, the last line confirms that the two $h(t)$ channels are in phase where the coherence is good enough to measure the phase.

As another validation, the NE PCal can be used, but in this case it is expected to have phase opposition between the NE PCal laser power and $h(t)$. Figure 6 (right column) confirms it is the case.

As continuous monitoring of the sign of $h(t)$, the PCal permanent lines injected at 36.5 Hz and 34.5 Hz on WE and NE PCal respectively are used. The package TFMoni is used for this purpose. The transfer functions from the PCal injected $h(t)$ channel (V1:PCAL_WEB_PD2_hpcal) to the raw $h(t)$ are computed online and generate in particular the monitoring channels TFMoni_WEMIR_HREC_HPCAL2_35_Cohe,Phase, sampled at 1 Hz[2]. The figures 7 and 8 show the time series of the phase and coherence, and distribution of the phase, over one month and over a lock segment. It confirms again that the phase is close to 0 from the injected $h(t)$ to the reconstructed $h(t)$ (hence with good sign). In addition, they show the time stability of the phase to be within 20 mrad, compatible with statistical fluctuations for permanent lines of signal-to-noise ratio of about 50.

[2] Since the sensing delay of the PCal cannot be included when computing the channel V1:PCAL_WEB_PD2_hpcal in Acl, the delay (122 µs)is taken into account in TFMoni.

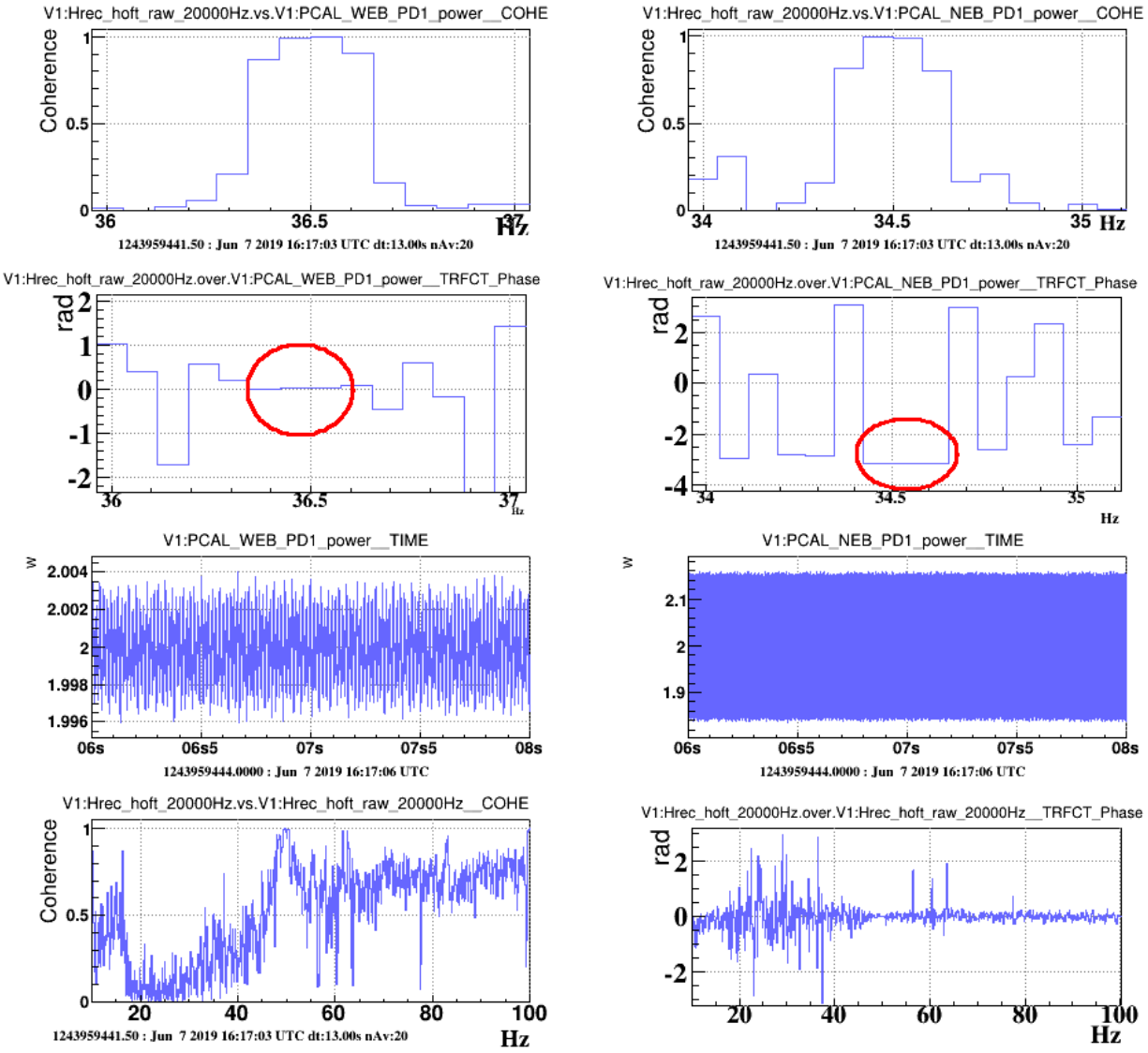

Figure 6: Validation of the sign of $h(t)$. The first two lines show the coherence and phase of the transfer function from the PCal power to the $h(t)$ channel including hardware injections (i.e. from PCAL_WEB_PD1_power to Hrec_hoft_raw_20000Hz). Left for WE and right for NE PCal. The phase points with good coherence at the PCal calibration line frequency are highlighted. The third line shows the time series of the PCal sensing channels, which give positive values. The last line shows the coherence and phase of the transfer function from Hrec_hoft_raw_20000Hz to Hrec_hoft_20000Hz: they are indeed in phase.,

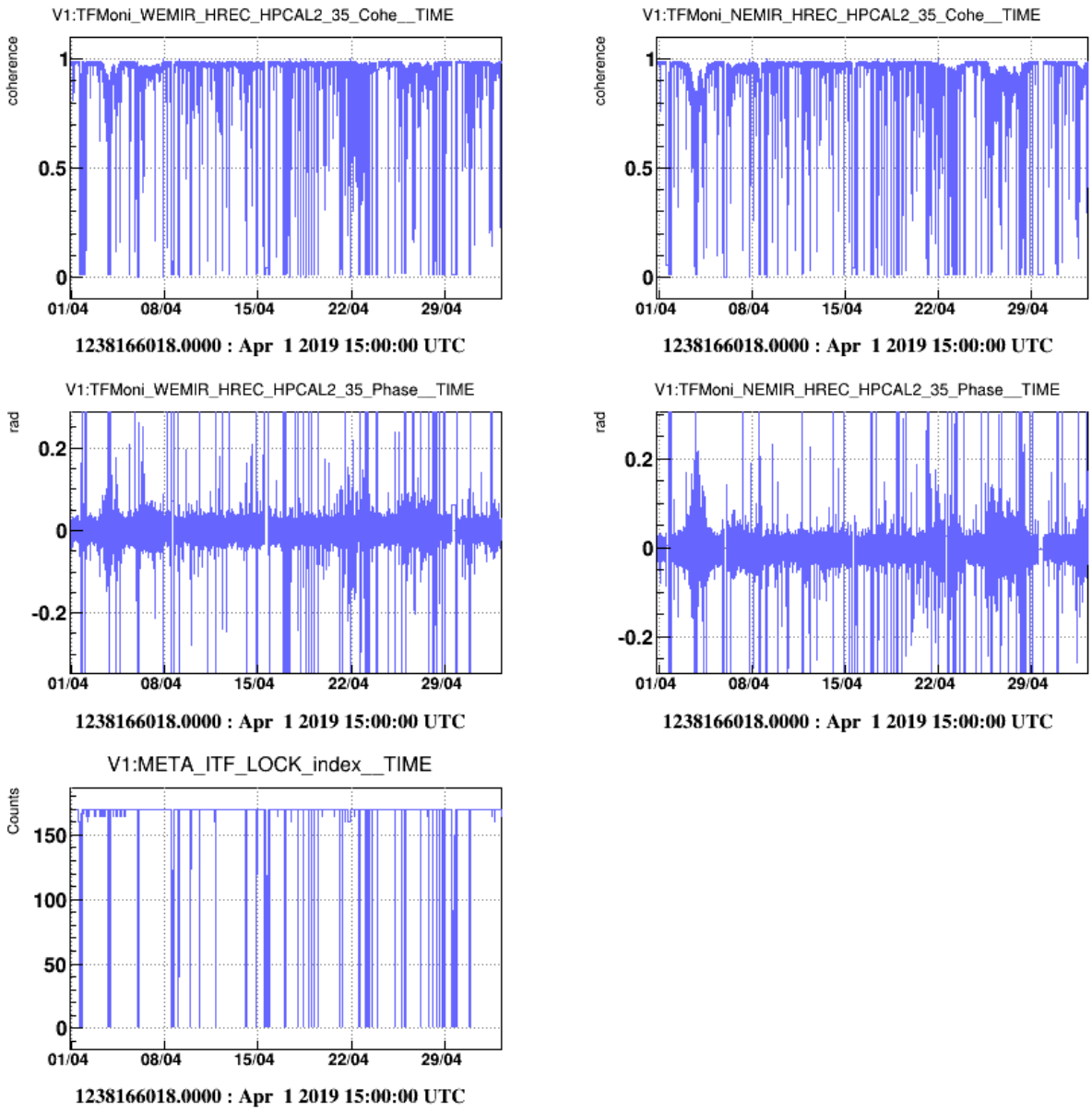

Figure 7: Monitoring of the sign of $h(t)$ with the photon calibration permanent lines during a month (April 2019).. The last line shows the time series of ITF lock index for reference. The first lines show the Time series of the coherence (top) and phase (middle) of the transfer functions at the frequency of the permanent line from the injected PCal $h(t)$ signal to the reconstructed raw $h(t)$ signal (left for WE and right for NE).

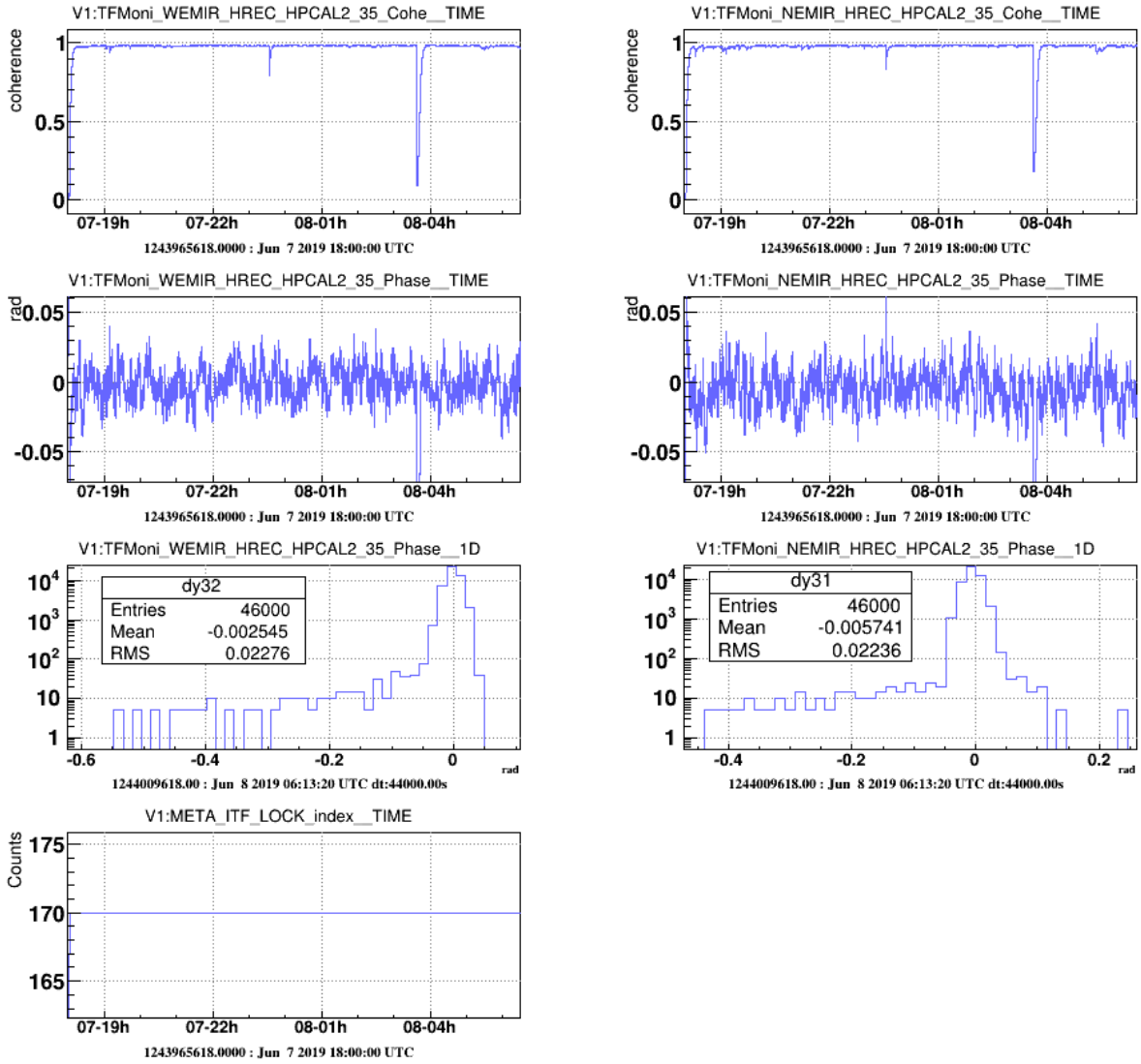

Figure 8: Monitoring of the sign of $h(t)$ with the photon calibrators during a lock segment on June 7th 2019. The last line shows the ITF lock index for reference. First and second lines show the time series of the coherence (first line) and phase (second lines) of the transfer functions from the injected PCal $h(t)$ signal to the reconstructed raw $h(t)$ signal (left for WE and right for NE). The third line shows the distribution of the phase (zoomed without a few outliers at the time of low coherence).

4.2 Validation of $h(t)$ with hardware injections

As usual, the $h(t)$ reconstruction is validated comparing the reconstructed channel to a known excitation on NE or WE mirrors.. Different actuators have been used to inject the known excitations: photon calibrators and electro-magnetic actuators[3].

For every type of injections, weekly measurements were done, injecting either a series of lines, or a broadband noise. The transfer functions from the calibrated excitation, h_{inj} to the reconstructed raw channel h_{raw} were computed. Their modulus and phase are expected to be around 1 and 0 respectively.

The results computed with injections via the photon calibrators and via the electromagnetic actuators are shown in the next two sections respectively. For each of the actuator, we give:

- the superposition of all the weekly measurements,
- for better visibility of the stability of the measurements, the measurements at some frequencies (around 35, 75, 165, 410, 810 and 1260 Hz) are given as a function of time in appendix A,
- for every injected frequencies, we estimate a systematic uncertainty from the small time variations that are observed,
- finally, we average the weekly measurements.

The data used here are from the beginning of the O3 run up to 7th June 2019. With weekly measurements, and some skipped calibration at the begnning of O3, the data are between April 17th and June 5th 2019 (GPS 1239540000 to 1243790000).

4.2.1 Validation of $h(t)$ with hardware injections using photon calibrators

The weekly measurements of the transfer functions h_{raw}/h_{inj}^{pcal} are shown in figure 9 for the WE and NE PCal injections: the measurements are well superposed and reproducible for excitations between 10 Hz and 1700 Hz.

To better check their time evolution, the modulus and phase is shown as a function of time at six different frequencies, in figures 18 and 19: it highlights the presence of small time variations.

To quantify these time variations, we used the same method as described in [5]: since the time variations are small, the data has been time-averaged. Then, the error bars of the individual (weekly) data points have been increased up to reaching a χ^2 probability of 5%. The results are shown on figure 10: above 20 Hz, systematic uncertainties of lower than 0.3% and

[3] Excitation using the NE Newtonian calibrator have also been injected but not yet analysed

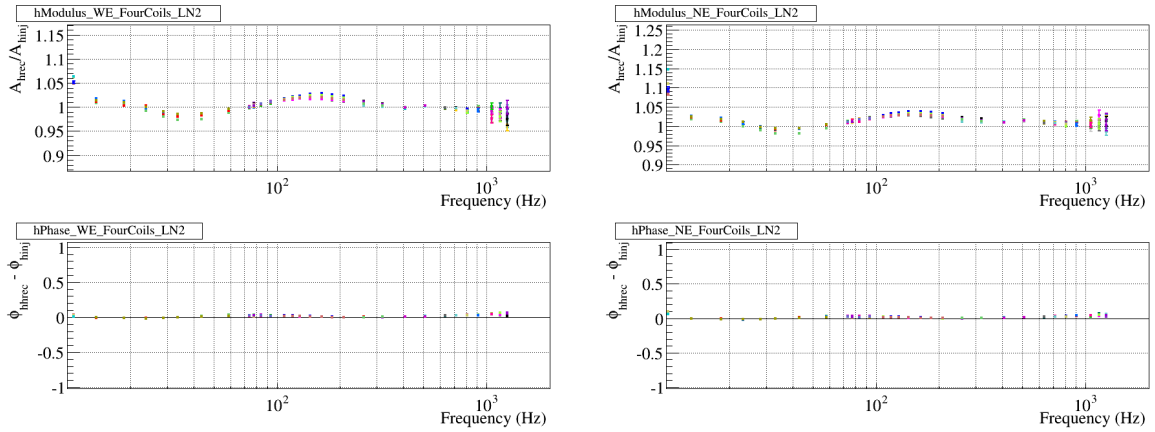

(a) WE PCal injections

(b) NE PCal injections

Figure 9: Comparison of the reconstructed raw $h(t)$ vs the $h(t)$ injected with the WE and NE PCals. Every weekly measurements are shown in a different color.

3 mrad are estimated on the modulus comparison and on the phase comparison respectively. Around 1 kHz, statistical uncertainties are larger and hide any time variation. The data looks more stable in the range from 400 Hz to 1 kHz. Around 10 Hz, the time variations are larger.

Since the time variations are small, the weekly measurements have been averaged to reduce the statistical uncertainties. The average of the weekly measurements of the transfer functions h_{raw}/h_{inj}^{pcal} are shown on figure 11. The modulus is well around 1, within better than 3% above 20 Hz. The phase is well around 0, within better than 30 mrad up to 800 Hz, with an indication for a 6 µs advance of h_{raw} compared to h_{inj}^{pcal} at high frequency.

Below 20 Hz, a larger difference is seen in amplitude (up to 10%) and the phase does not converge towards 0. This behavior has to be investigated but has no impact on the current $h(t)$ channel for data analysis above 20 Hz.

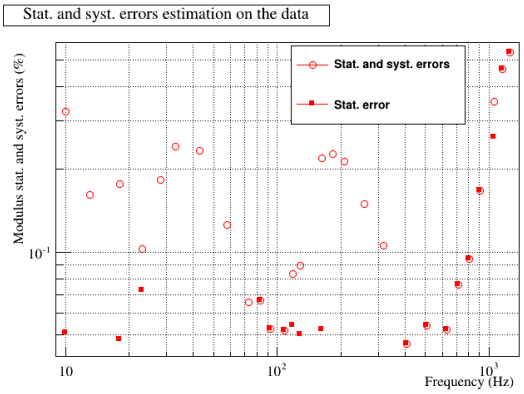

(a) WE PCal injections: modulus

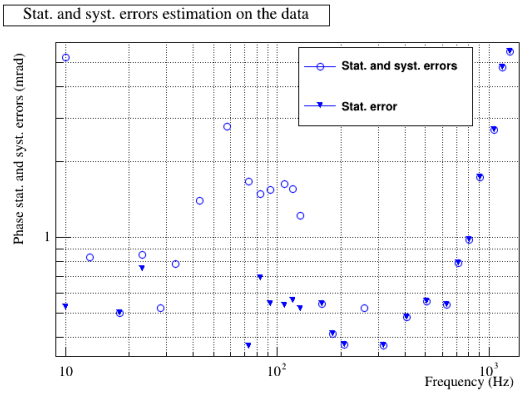

(b) WE PCal injections: phase

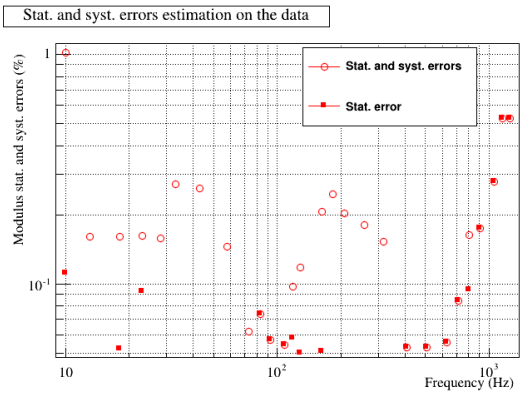

(c) NE PCal injections: modulus

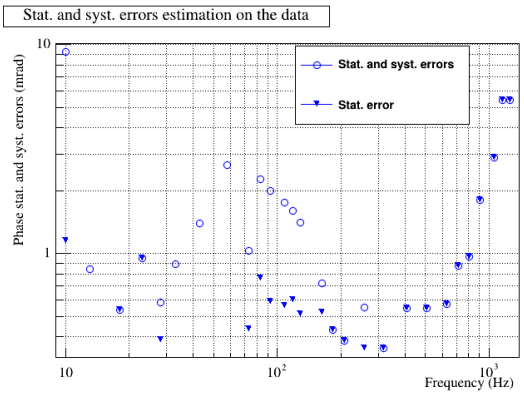

(d) NE PCal injections: phase

Figure 10: Summary of the stat. and syst. uncertainties estimated from the time stability of the reconstructed raw $h(t)$ vs the $h(t)$ injected with the NE and WE photon calibrators. For every frequency, the stat. uncertainty is shown as a colored marker, and the sum of stat. and additional syst. uncertainty is shown as an empty marker. Both are superposed when there is no hint for time variation, which is mainly the case above 400 Hz.

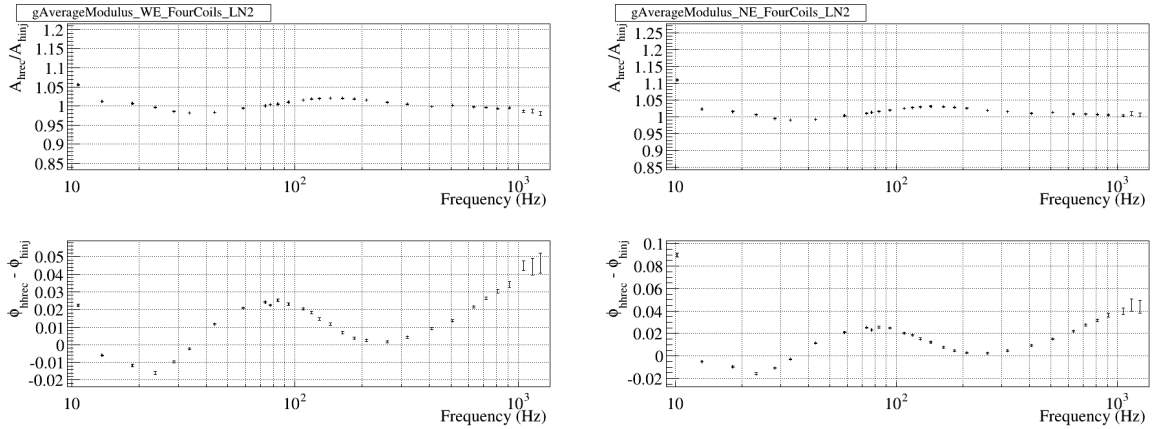

(a) WE PCal injections

(b) NE PCal injections

Figure 11: Comparison of the reconstructed raw $h(t)$ vs the $h(t)$ injected with the WE and NE PCals. This is the average of weekly measurements.

4.2.2 Validation of $h(t)$ with hardware injections using electromagnetic actuators

The weekly measurements of the transfer functions h_{raw}/h_{inj}^{EM} are shown in figure 12 for the WE and NE electromagnetic actuator injections: the measurements are well superposed and reproducible for excitations between 10 Hz and 1700 Hz.

To better check their time evolution, the modulus and phase is shown as a function of time at six different frequencies, in figures 20 and 21: it highlights the presence of small time variations.

To quantify these time variations, we used the same method as described in the previous section. The results are shown on figure 13: above 20 Hz, systematic uncertainties of lower than 0.3% and 3 mrad are estimated on the modulus comparison and on the phase comparison respectively. Around 10 Hz, the time variations are larger.

Since the time variations are small, the weekly measurements have been averaged to reduce the statistical uncertainties. The average of the weekly measurements of the transfer functions h_{raw}/h_{inj}^{EM} are shown on figure 14. The behavior is very close to the one obtained using the PCal actuator injections and the same conclusions can be done.

4.2.3 Remarks on $h(t)$ validation with weekly hardware injections

Four different actuators (NE and WE mirrors, and electromagnetic and photon calibrator actuators) have been used to validate $h(t)$ reconstruction. They all find similar results: the modulus is well around 1, within better than 3.5% above 20 Hz ; the phase is well around 0, within better than 30 mrad up to 800 Hz, with an indication for a 6 µs advance of h_{raw} compared to h_{inj}^{pcal} at high frequency. Below 20 Hz, a larger difference is seen in amplitude (up to 10%) and the phase does not converge towards 0. This behavior has to be investigated but has no impact on the current $h(t)$ channel for data analysis above 20 Hz.

The fact that hardware injections using four different actuators give the same stable results indicate that:

- the measured frequency-dependent shape must come from a bias is $h(t)$ and not from errors in the four h_{inj} estimations.
- this biais is stable in time within better than 0.3% and 3 mrad.

The main difference is the behavior of the modulus at high frequency which differ by up to 5% between the actuators. This has to be investigated. However, all the modulus are inside the ±3.5% band for all the actuators.

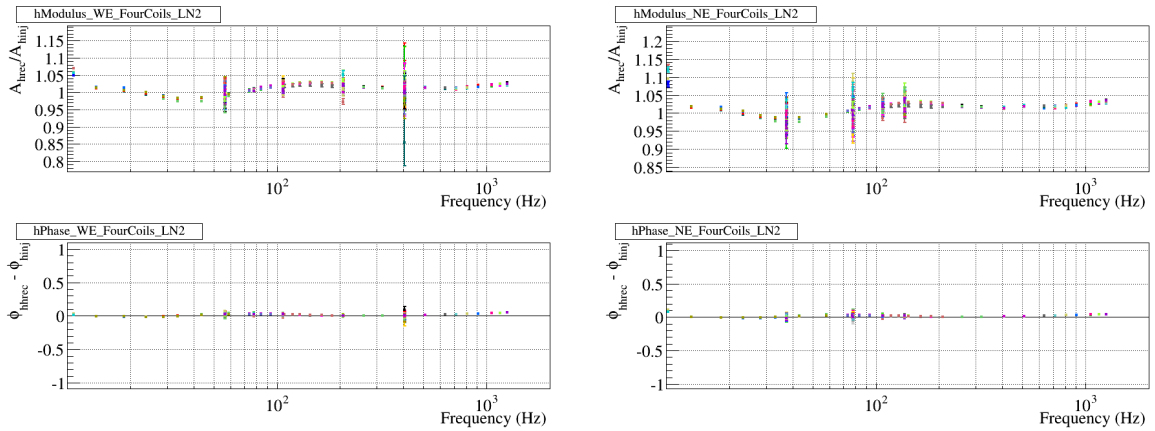

(a) WE EM injections

(b) NE EM injections

Figure 12: Comparison of the reconstructed raw $h(t)$ vs the $h(t)$ injected with the WE and NE electromagnetic actuators. Every weekly measurements are shown in a different colors.

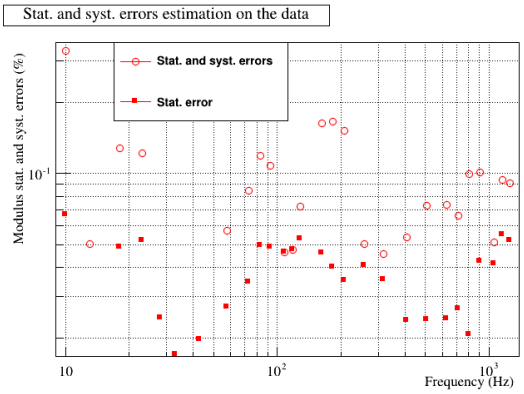

(a) WE EM injections: modulus

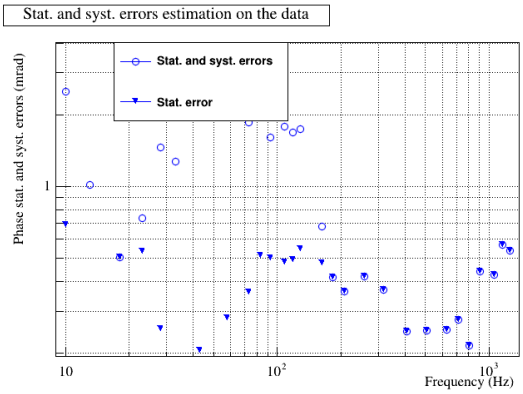

(b) WE EM injections: phase

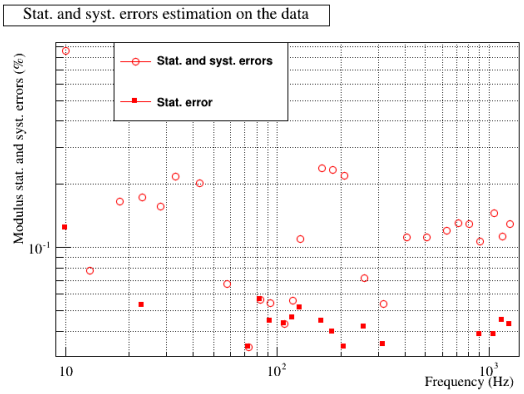

(c) NE EM injections: modulus

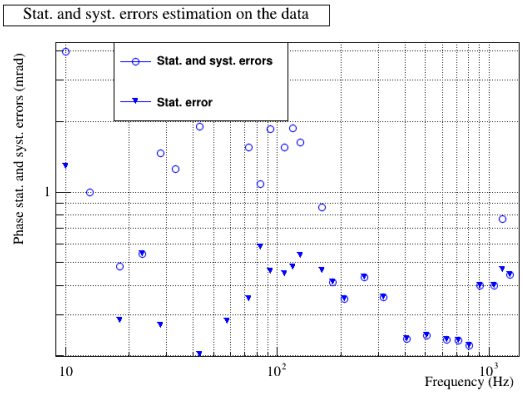

(d) NE EM injections: phase

Figure 13: Summary of the stat. and syst. uncertainties estimated from the time stability of the reconstructed raw $h(t)$ vs the $h(t)$ injected with the NE and WE electromagnetic actuators. See text for details.

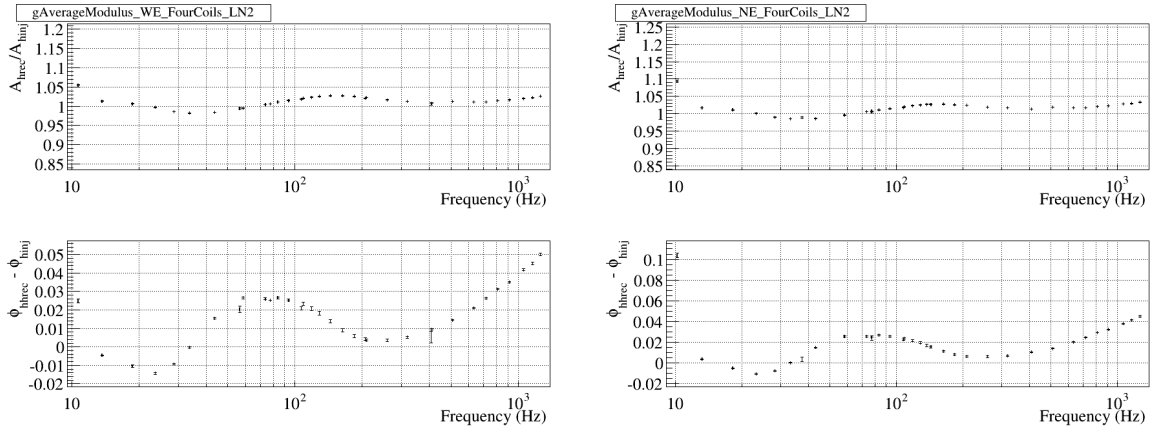

(a) WE EM injections

(b) NE EM injections

Figure 14: Comparison of the reconstructed raw $h(t)$ vs the $h(t)$ injected with the WE and NE electromagnetic actuators. This is the average of weekly measurements.

4.2.4 Monitoring of $h(t)$ stability with permanent hardware injections

Permanent hardware injections of lines have been setup before the start of O3 in order to monitor the calibration and reconstruction continuously. Hardware injections are injected via either NE or WE mirrors, and via either the electromagnetic or photon calibrator actuators. Having different source of injections permits to monitor the stability of relative calibration between actuators.

The table 1 summarizes the injected frequency and actuators, and gives their typical signal-to-noise ratio in DARM signal for FFTs length of 10 s. The TFMoni tool is running online to compute the transfer function from the injected signal (calibrated in h_{inj} to the reconstructed channel h_{raw}). It produces time series of the modulus, phase and coherence of the transfer functions at the injected frequencies. The figures 15 and 16 show the distributions of the modulus and phase computed between 11th April and 20th June 2019 when the ITF was locked[4]. The distributions are Gaussian and their RMS (between 0.6% and 3% in modulus) matches the statistical fluctuations expected due to their signal-to-noise ratio. Hence it is not needed to call for significant time variations to explain the distributions[5].

Only around 405 Hz the distributions are not Gaussian and show tails, but they are still well centered around correct values close to 1 in modulus and 0 in phase. This effect has to be investigated. One possible explanation could be that some noise is going up and down around that line, reducing its signal-to-noise ratio when the noise is higher, hence adding statistical variations at that time.

To conclude, the continuous monitoring using these hardware injections confirms the stability of both the four actuator responses and the h_{raw}/h_{inj} ratio within their statistical uncertainties, i.e. better than 0.6% to 3% in modulus and better than 6 mrad to 28 mrad in phase. This is consistent with the weekly measurements described in previous sections: with larger signal-to-noise ratio, small time variations were estimated to 0.3% and 3 mrad, too small to be observed with the current continuous monitoring.

[4] The actuation models in TFMoni were not udpated from the very beginning of O3 on April 1st, hence the check was started from April 11th

[5] In case of stochastic time variations of the ratio h_{rec}/h_{inj}, we expect a Gaussian distribution but with RMS higher than expected from line SNR ; Non-Gaussian distribution, still centered on the expected value, can be caused by fluctuation of the line SNR, i.e. variation of the detector noise around the line.

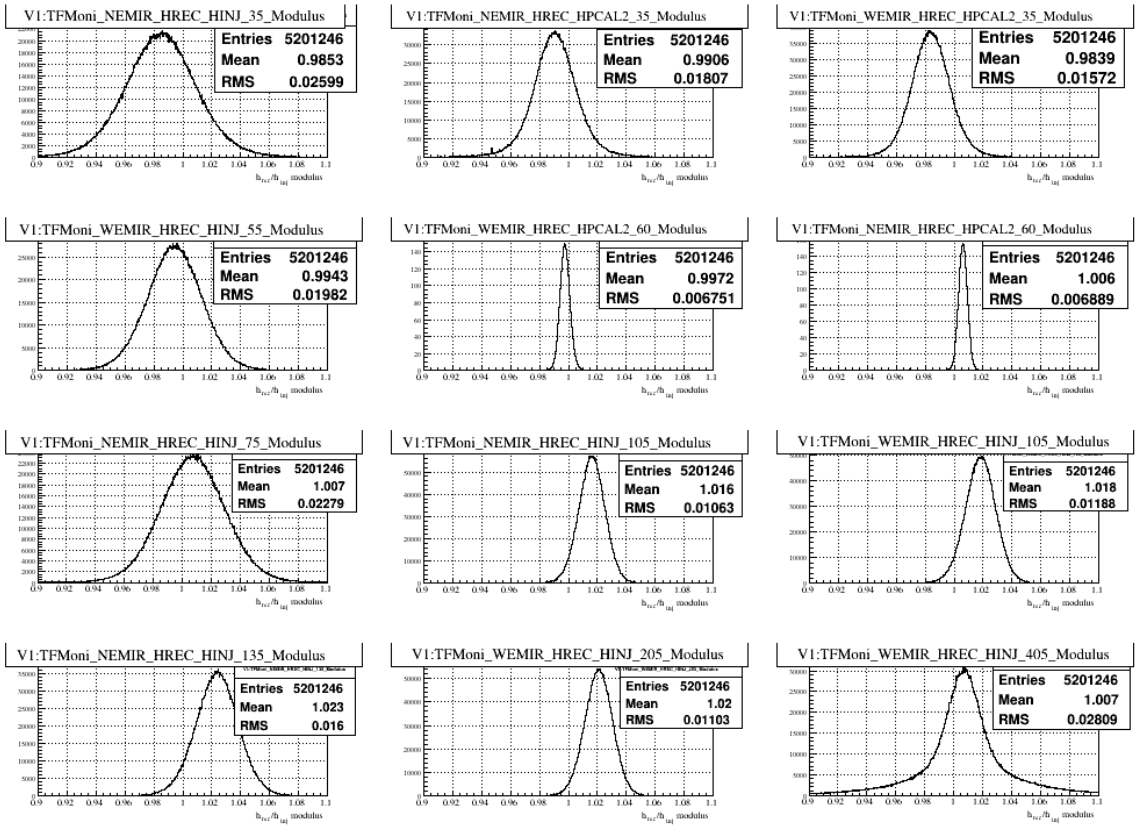

Figure 15: Distribution of the modulus of h_{raw}/h_{inj} computed on permanent calibration lines injected as hardware injections using the electromagnetic or PCal actuators on NE or WE mirrors. The measurements are from April 17th to 20 June 2019, selecting time when the ITF was locked.

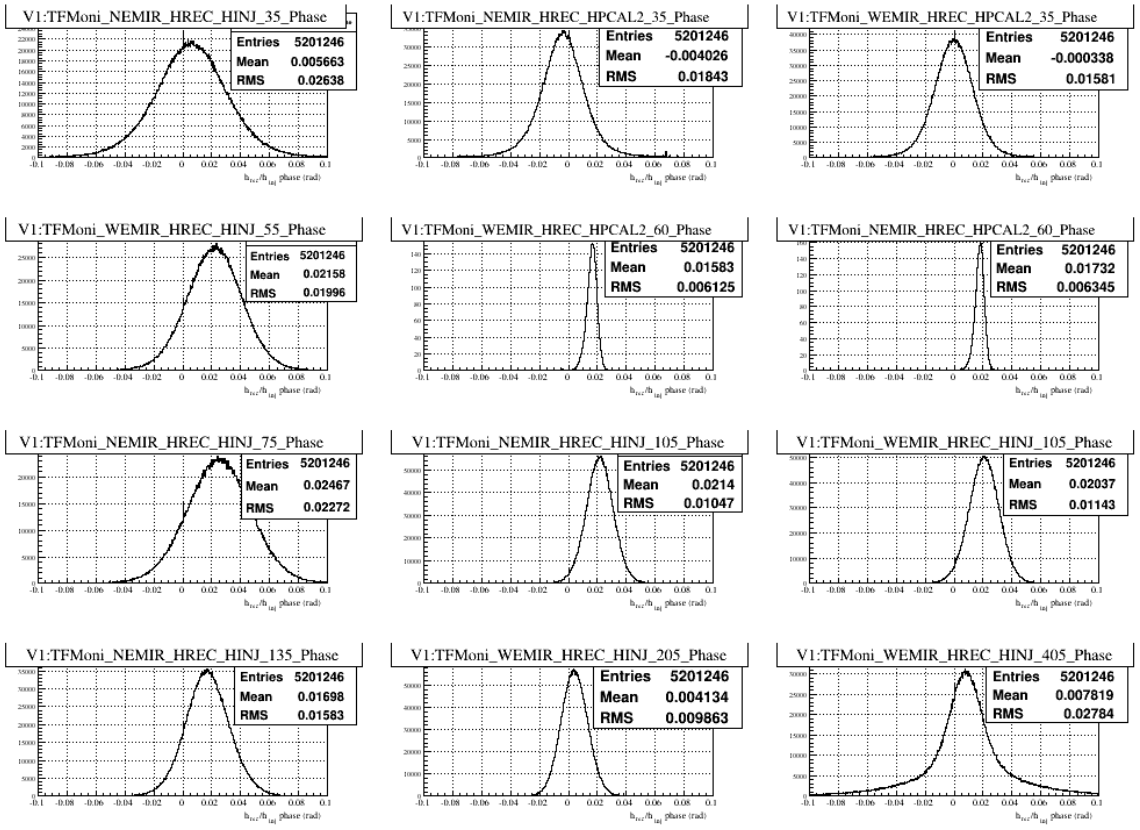

Figure 16: Distribution of the phase of h_{raw}/h_{inj} computed on permanent calibration lines injected as hardware injections using the electromagnetic or PCal actuators on NE or WE mirrors. The measurements are from April 17th to 20 June 2019, selecting time when the ITF was locked.

Frequency (Hz)	Mirror	Actuator	Typical SNR
36.5	WE	PCAL	30
34.5	NE	PCAL	30
37.5	NE	EM	20
56.5	WE	EM	20
60.5	WE	PCAL	130
63.5	NE	PCAL	130
77.5	NE	EM	20
106.5	WE	EM	60
107.5	NE	EM	60
137.5	NE	EM	40
206.5	WE	EM	50
406.5	WE	EM	40

Table 1: Summary of the permanent hardware injections of calibration lines. For each frequency, the excited mirror (WE or NE) and actuator (EM or PCal) is given. The typical signal-to-noise ratio of the line above the noise spectrum is also given.

4.2.5 Estimation of $h(t)$ uncertainties

The weekly averaged h_{raw}/h_{inj} transfer functions described in the previous sections are superposed in the figure 17, showing only statistical uncertainties.

It confirms that the four different checks give the same results, with some discrepancy on the amplitude check at high frequency. This behavior is under investigation[6].

Above 20 Hz, these measurements are used to estimate the uncertainty bands at ±3.5% in amplitude and ±30 mrad in phase, represented by the red lines. In addition, a timing uncertainty of about 7 µs must be added to explain the phase increase at high frequency[7].

In addition, the systematic uncertainties from the actuator models used to estimate the different h_{inj} must be added. The systematic uncertainty on the modulus calibration using the PCal method is estimated to 1.9% [9].

As an independent comparison, the free swinging Michelson technic has also been used for EM actuator calibration. The systematic uncertainty on the calibration using this technic is es-

[6] One current investigation is on the PCal mechanical model, which vis not accurate around 1 kHz since there is a notch around 2 kHz (due to the PCal exciting the mirror drum mode) that was not precisely tuned at the beginning of O3. It probably creates a biais that over-estimate h_{pcal} by about 4%. In this case, the green and blue curve would get close to the red and yellow ones. This would reduce the discrepancy between the measurements, but still would indicate a few percent biais of $h(t)$ around 1 kHz.

[7] A delay of about 10 µs is probably what is expected in this measurement due to the difference between the simple cavity pole assumption and the real optical response model described in note [8]. This is under investigation, but it would imply that the delay uncertainty would be $(-)3$ µs instead of 7 µs.

timated to 1% to 2% [5]. And the results of both calibration technics (PCal and free Michelson) are consistent within better than 2.6% [6], hence within the systematic uncertainties. Using 3.5% as an estimate of the systematic uncertainty on the h_{inj} signals, the sum in quadrature gives 4.4%.

Finally, we give the systematic uncertainty on the online $h(t)$ to be $\pm 5\%$ since some caution must be kept for possible time variations of calibration parameters that may be observed when analysing the calibration data of a longer period of O3.

For the phase, the systematic uncertainties from time variations and PCal to free swinging Michelson method differences are negligible compared to 30 mrad. For the timing, the uncertainties are of the order of 3 µs on the PCal actuators [9], and the comparison of PCal and free swinging Michelson technics [6] shows an agreement within 1 µs. The uncertainty on the B1 photodiode timing [5] is estimated to 2.5 µs.

Finally, we give the systematic uncertainty on the online $h(t)$ phase and timing to be ± 35 mrad and 10 µs again keeping some safety margin waiting for longer term .checks of calibration stability.

To conclude, the systematic uncertainties on the online $h(t)$ channel provided at the beginning of O3, in the range from 20 Hz to 2 kHz, are estimated to:

- $\pm 5\%$ in amplitude
- ± 35 mrad in phase
- ± 10 µs in timing

5 Plans for reprocessing and HRec improvements

As stated early 2019, we planned a single reprocessing at the end of O3a if needed, and not intermediate reprocessing, except in case of clear calibration error of course. As of September 2019, it seems that this is not really compatible with the analysis timeline since PE is run on every events much before the end of O3a, so we may want to change this in the future. However, for now, we have checked that the calibration has been stable from April to end of August, so we do not have better calibration models to significantly improve the $h(t)$ compared to the online version. As a consequence, the online $h(t)$ is the one to be used for data analysis of O3a.

In the future, in case of an exceptional event in a period with known improved calibration models, a fast reprocessing of $h(t)$ can be planned.

One issue with the current online $h(t)$ are some 500 s periods with bad noise subtraction after glitches, inducing few Mpc loss during 500 s. As no GW event happened during such a period,

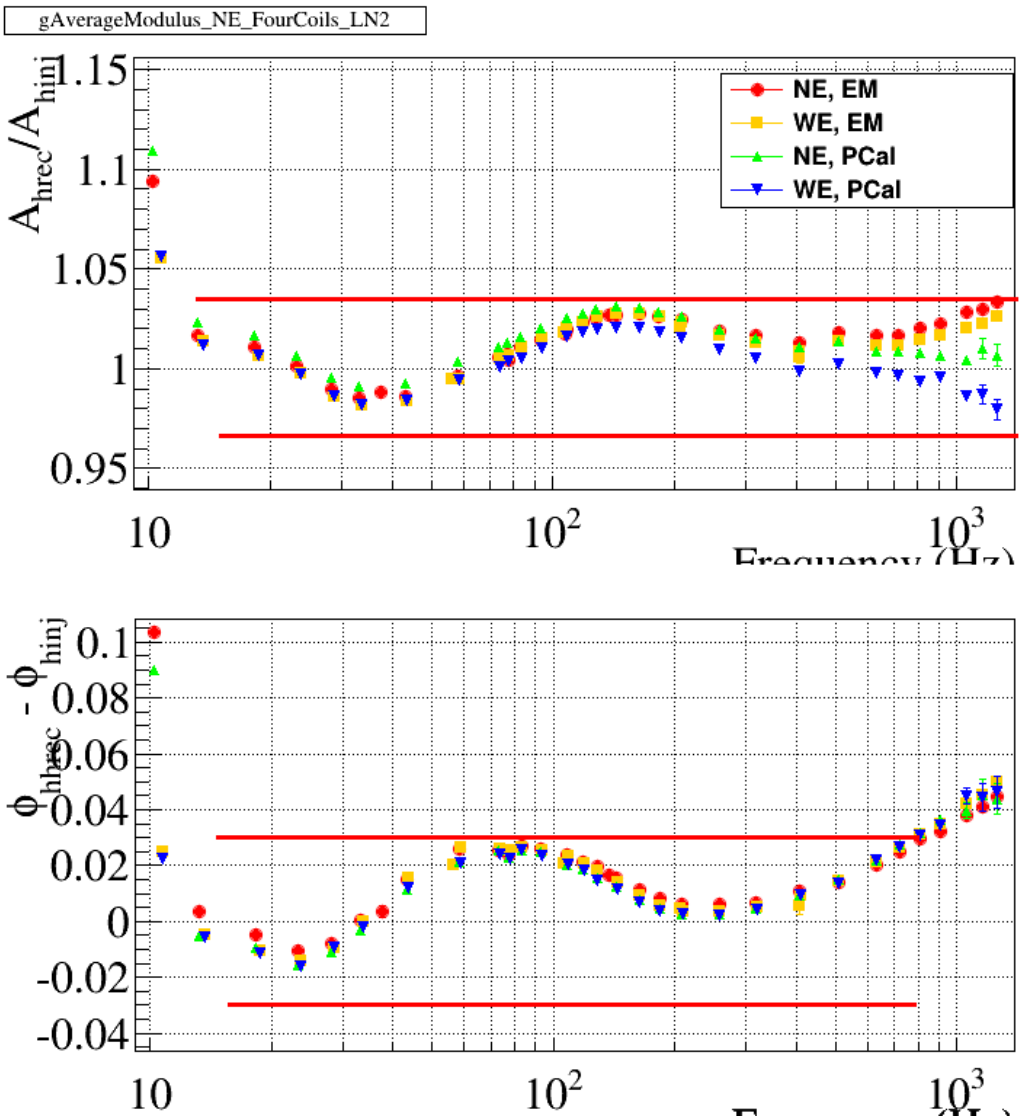

Figure 17: Superposition of the weekly averaged h_{raw}/h_{inj} transfer functions measured with different injections on NE and WE EM and PCal actuators. The red lines indicate the bands that are used to estimate the $h(t)$ uncertainties.

this is not an issue for data analysis of the detected events. The effect for continuous searches is limited since it affects only a small fraction of the data. However, some work is on-going to fix this issue. Our plan is to update the online version for future data, not to reprocess O3a data.

References

[1] E. Estevez, L. Rolland, *et al.*, "Calibrating end mirror and marionette actuators with photon calibrators at the beginning of o3," *Virgo note*, vol. VIR-0466B-19, May 2019.

[2] B. Mours, L. Rolland, *et al.*, "V1O2Repro1A $h(t)$ reprocessing for Virgo O2 data," *Virgo note*, vol. VIR-0706B-17, Sept. 2017.

[3] E. Estevez, L. Rolland, *et al.*, "V1o2repro2a h(t) reprocessing for virgo o2 data," *Virgo note*, vol. VIR-0014AA-18, Jan. 2018.

[4] T. Accadia, (Virgo collaboration), *et al.*, "Reconstruction of the gravitational wave signal h(t) during the virgo science runs and independent validation with a photon calibrator," *Class. Quantum Grav.*, vol. 31, no. 16501, 2014. (arXiv:1401.6066).

[5] L. Rolland *et al.*, "Advanced virgo calibration for o3:calibration based on free swinging michelson," *Virgo note*, vol. VIR-0529A-19, May 2019.

[6] E. Estevez, L. Rolland, *et al.*, "Comparing the end mirror actuator models derived from pcal and free swinging michelson measurements at the beginning of o3," *Virgo note*, vol. VIR-0544A-19, May 2019.

[7] B. O'Reilly *et al.*, *Convention for the Sign of the Calibration.* LIGO-T1000144-v1, 2010.

[8] L. Rolland, "Notes on single-pole cavity approximation and long-wavelength interferometer approximation," *Virgo note*, vol. VIR-0530A-15, Dec. 2015.

[9] E. Estevez, L. Rolland, *et al.*, "Calibration of the advanced virgo photon calibrators for o3," *Virgo note*, vol. VIR-0397B-19, Apr. 2019.

A Validation of $h(t)$ with hardware injections: stability

In this appendix, the modulus and phase of h_{raw}/h_{inj} is shown at six frequencies for all the weekly measurements between April and 5 June 2019. The $h_{inj}(t)$ was injected via NE PCal, WE PCal, NE EM actuator or WE EM actuator, and the corresponding data are shown in figures 18, 19, 20 and 21.

For every measurement, the statistical uncertainties are shown, coming from the coherence between the injected signal and the reconstructed $h(t)$. The red line indicates the weighted average of the data. The average value and its statistical uncertainties, as well as the χ^2/ndf of the fit, are given.

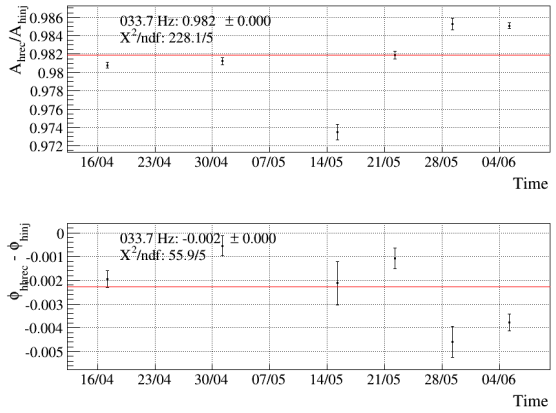

(a) WE PCal injections at 33.7 Hz

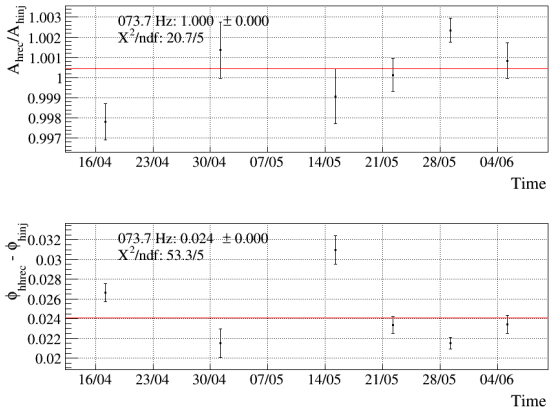

(b) WE PCal injections at 73.7 Hz

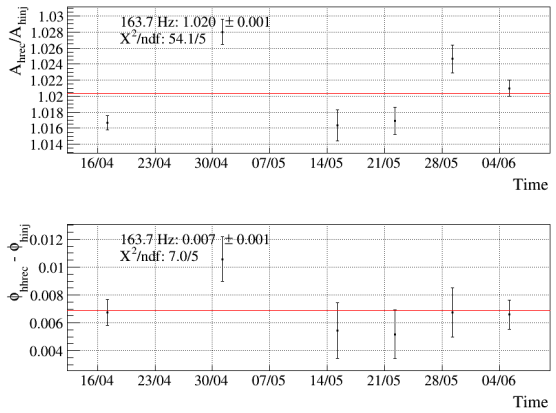

(c) WE PCal injections at 163.7 Hz

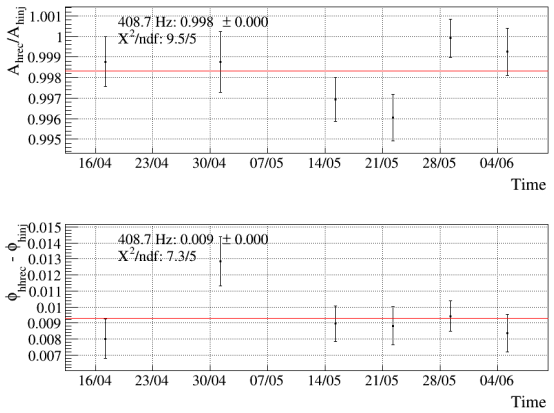

(d) WE PCal injections at 408.7 Hz

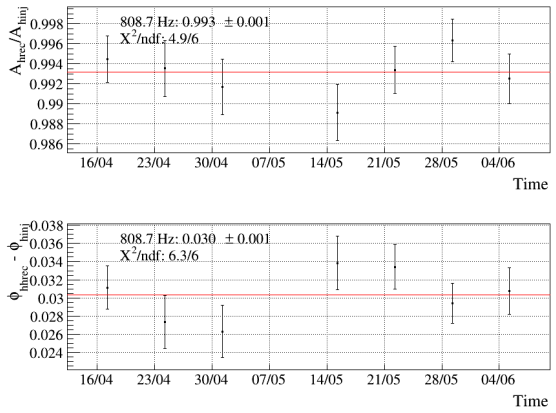

(e) WE PCal injections at 808.7 Hz

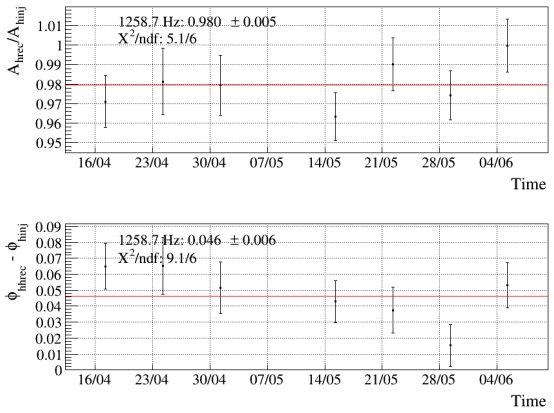

(f) WE PCal injections at 1258.7 Hz

Figure 18: Comparison of the reconstructed raw $h(t)$ vs the $h(t)$ injected with the WE PCal. Weekly measurements, shown at different frequencies. See text for details.

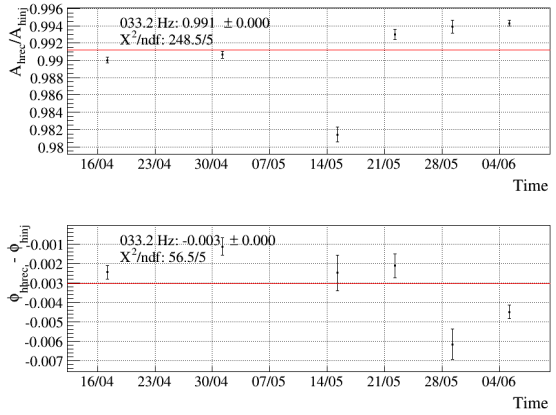

(a) NE PCal injections at 33.2 Hz

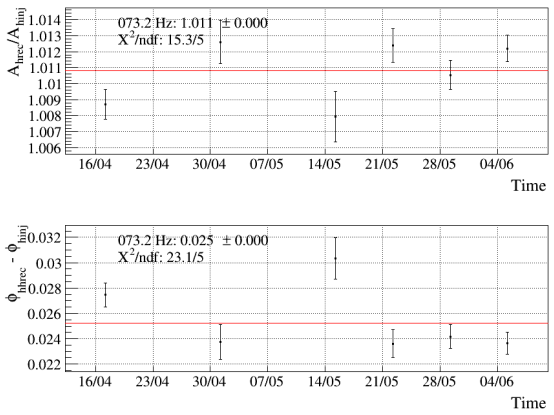

(b) NE PCal injections at 73.2 Hz

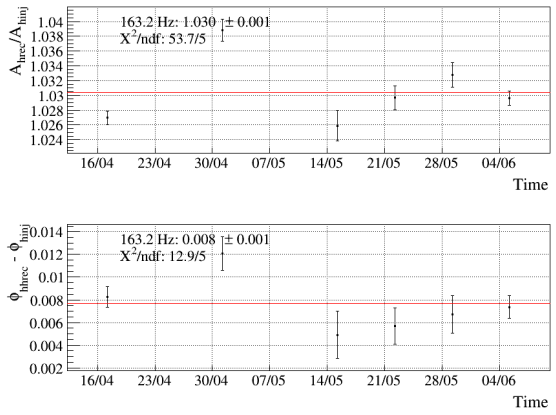

(c) NE PCal injections at 163.2 Hz

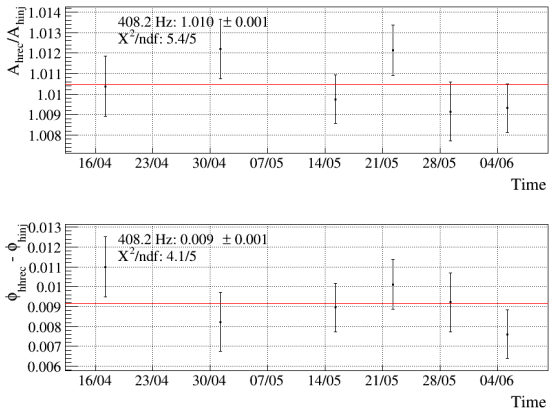

(d) NE PCal injections at 408.2 Hz

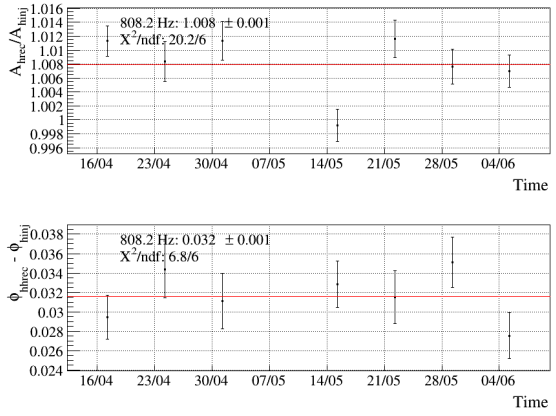

(e) NE PCal injections at 808.2 Hz

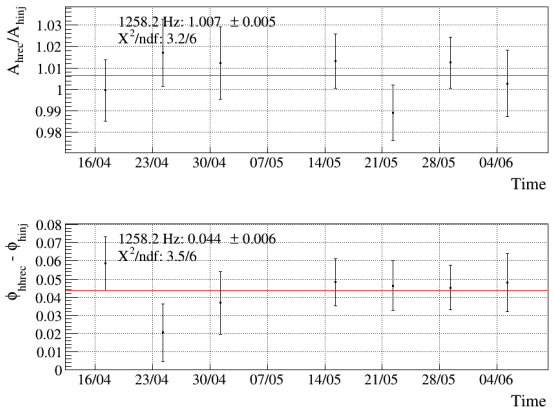

(f) NE PCal injections at 1258.2 Hz

Figure 19: Comparison of the reconstructed raw $h(t)$ vs the $h(t)$ injected with the NE PCal. Weekly measurements, shown at different frequencies. See text for details.

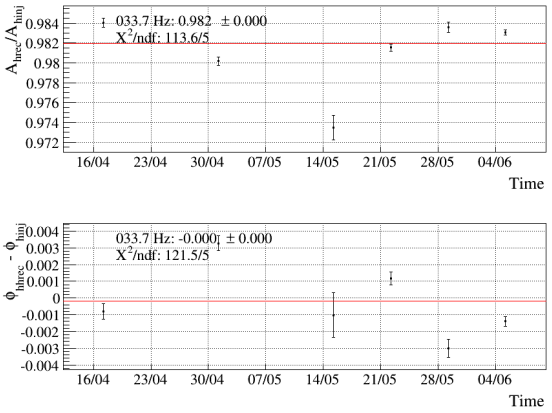

(a) WE EM injections at 33.7 Hz

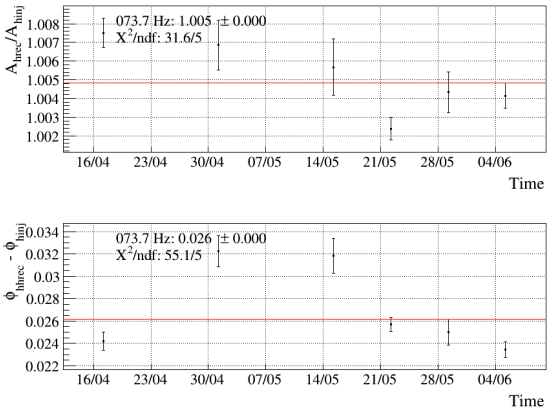

(b) WE EM injections at 73.7 Hz

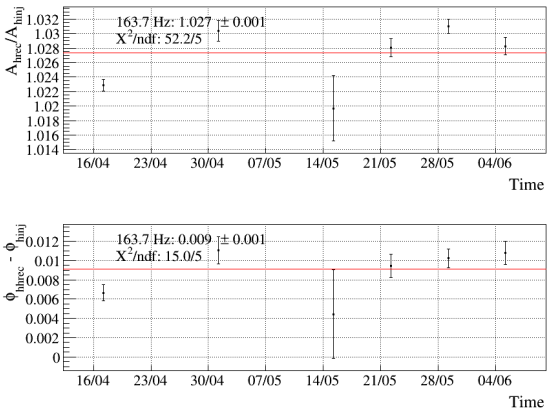

(c) WE EM injections at 163.7 Hz

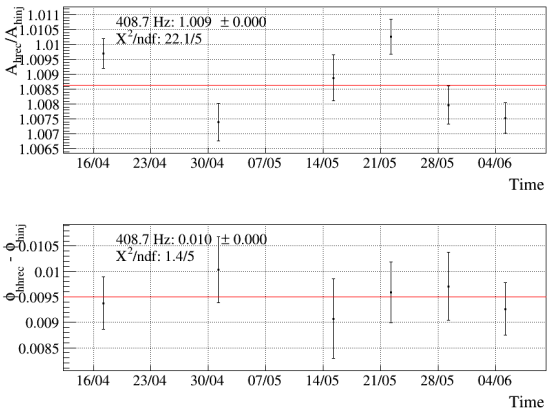

(d) WE EM injections at 408.7 Hz

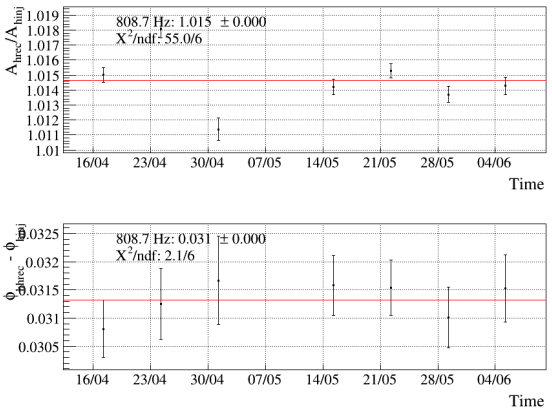

(e) WE EM injections at 808.7 Hz

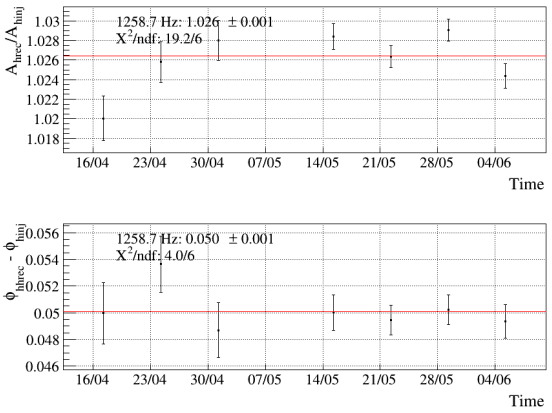

(f) WE EM injections at 1258.7 Hz

Figure 20: Comparison of the reconstructed raw $h(t)$ vs the $h(t)$ injected with the WE electromagnetic actuator. Weekly measurements, shown at different frequencies. See text for details.

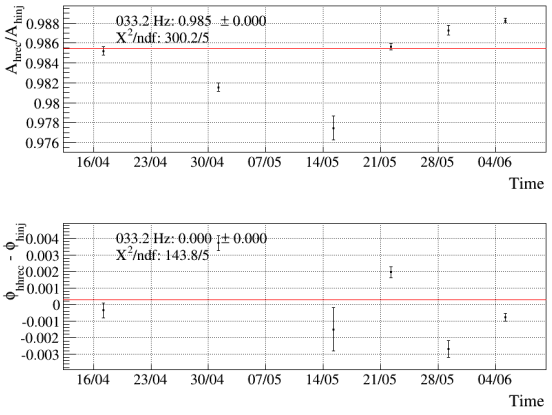

(a) NE EM injections at 33.2 Hz

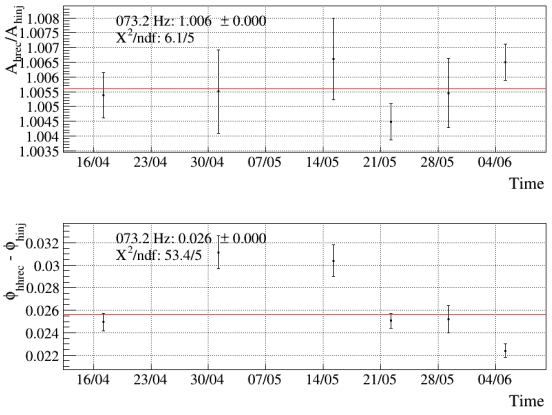

(b) NE EM injections at 73.2 Hz

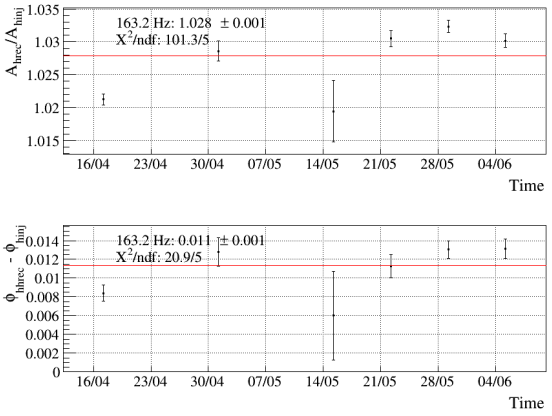

(c) NE EM injections at 163.2 Hz

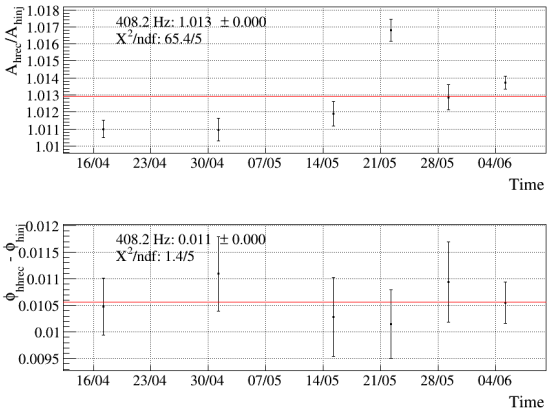

(d) NE EM injections at 408.2 Hz

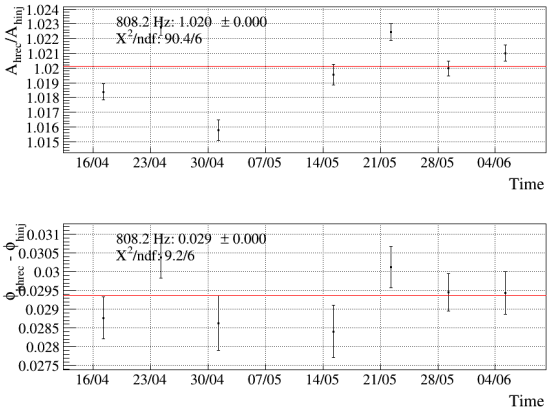

(e) NE EM injections at 808.2 Hz

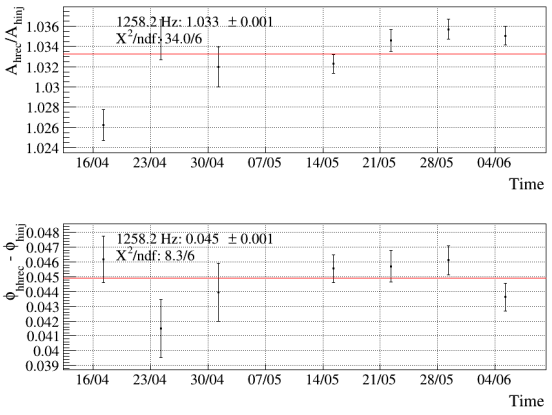

(f) NE EM injections at 1258.2 Hz

Figure 21: Comparison of the reconstructed raw $h(t)$ vs the $h(t)$ injected with the NE electromagnetic actuator. Weekly measurements, shown at different frequencies. See text for details.

B HRec configuration files used online

B.1 Main file: HRec.cfg

```
# Main priority
CFG_PRIO 0

# working directory path
CFG_PWD /virgoLog/VirgoOnline

CFG_SCHEDAFFINITY 13-31 # with Cfg v8r06


CFG_NOFILESAVE
CFG_NODBSAVE             # No commit into Db


DEBUG 3

define HREC_PREFIX V1:Hrec
OUTPUT_PREFIX HREC_PREFIX

##-------------------------------------------------------Fd
FDIN_DIR  /dev/shm/VirgoOnline/FbmAlp -1
FDIN_TAG  "V1:Sc_*_MAR_Z_CORR V1:Sc_*_MIR_Z_CORR V1:CAL_*_MIR_Z_NOISE V1:PCAL_*_PD*_hpcal V1:SDB2_B1*_PD*_Blended V1:META_ITF_LOCK V1:DQ_META V1:SAT V1:SIB2_B2_8MHz_I V1:SPRB_
FDIN_FRAME_DURATION 4
# FDIN_COMBINE_CHANNELS V1:B1 0.522 V1:SDB2_B1_PD1_Blended .478 V1:SDB2_B1_PD2_Blended
FDIN_COMBINE_CHANNELS V1:B1 0.495 V1:SDB2_B1_PD1_Blended 0.505 V1:SDB2_B1_PD2_Blended


FDOUT_FRAME_DURATION 1
FDOUT_RANGE_GATING_NEW HREC_PREFIX_hoft_16384Hz 1.4 10 32 0.6 0.25 0.3125 10
FDOUT_BITOP  V1:DQ_ANALYSIS_STATE_VECTOR HREC_PREFIX_STATE_VECTOR   AND 0xffff

/*
FDIN_ADD_SURROGATE_DQ_CHANNEL V1:DQ_VETO_MBTA   50 1 0 0 10 1.
FDIN_ADD_SURROGATE_DQ_CHANNEL V1:DQ_VETO_CWB    50 1 0 0 10 1.
FDIN_ADD_SURROGATE_DQ_CHANNEL V1:DQ_VETO_GSTLAL 50 1 0 0 10 1.
FDIN_ADD_SURROGATE_DQ_CHANNEL V1:DQ_VETO_OLIB   50 1 0 0 10 1.
FDIN_ADD_SURROGATE_DQ_CHANNEL V1:DQ_VETO_PYCBC  50 1 0 0 10 1.
*/
# Destination Cm name - channel tags - 0: CmSend, >0: queue size and CmPost - retry - <checksum>
#FDOUT_CM FbmSt  "#PROC V1:Hrec* V1:DQ_ANALYSIS_STATE_VECTOR #SER V1:Hrec* V1:DQ_*" 0 -1

# Compression type  - nbThread
FDOUT_COMPRESSION  8 0

FDOUT_FILE   /dev/shm/VirgoOnline/HRec/V1-Hrec 1  "#PROC V1:Hrec* V1:DQ_ANALYSIS_STATE_VECTOR #SER V1:Hrec* V1:DQ_*"
FDOUT_FILE_CHECKSUM 0
FDOUT_CLEAN_DIR /dev/shm/VirgoOnline/HRec 1 0 0.0 40

FDOUT_FILE   /dev/shm/VirgoOnline/HRecToSt/V1-Hrec 1  "#PROC V1:Hrec* #SER V1:Hrec* V1:DQ_*"
FDOUT_FILE_CHECKSUM 0
FDOUT_CLEAN_DIR /dev/shm/VirgoOnline/HRecToSt 1 0 0.0 40


PROCESSING_TAG HrecV0
##-------------------------------------------------------Some global parameters
MIN_LOCK_STATE 159
START_FRQUENCY 8.
FINESSE_REF 450
TIME_MARGIN_BAD_SNR 200
SHAPING_FILTER 1 20 3

##-------------------------------------------------------Subtraction of controls, Calibration and Noise channels
#--------------Remove  Main channels and define the raw channel before noise subtraction
include HRec_MainChannels_FromPCal.cfg

H_FREQUENCY 20000 HREC_PREFIX_hoft_raw_20000Hz


#--------------Remove  Noise channels and define the clean channel to be used for hrec checks and HWII use
include HRec_NoiseChannels.cfg

H_FREQUENCY 20000 HREC_PREFIX_hoft_clean_20000Hz


#--------------Remove  CAL channels
include HRec_CalChannels_FromPCal.cfg

##-------------------------------------------------------Optical gains
/* Calibration line frequencies have been changed on August 17, 2018:
```

```
NE is now 62.5  (was 63.3)  357.5 (was 358.3)
WE is now 61.5  (was 60.8)  356.5 (was 355.8)
BS is now 61.0  (was 62.8)  356.0 (was 357.8)
PR is now 63.0  (was 62.3)  358.0 (was 357.3)
-------------------------------------*/

#--------- this is to compute the optical gains with the usual permanent lines ---
GET_OGAIN 4 2 V1:Sc_NE_MIR_Z_CORR   62.5  10. V1:Sc_WE_MIR_Z_CORR   61.5  10. V1:Sc_BS_MIR_Z_CORR  61.0  10. V1:Sc_PR_MIR_Z_CORR  63.0 0.
GET_OGAIN_FREQ_BCKGRND 62 2
GET_OGAIN 4 2 V1:Sc_NE_MIR_Z_CORR  357.5  10. V1:Sc_WE_MIR_Z_CORR  356.5  10. V1:Sc_BS_MIR_Z_CORR 356.0  10. V1:Sc_PR_MIR_Z_CORR 358.0 0.
GET_OGAIN_FREQ_BCKGRND 357 2

#GET_OGAIN 3 2 V1:Sc_NE_MIR_Z_CORR   62.5  10. V1:Sc_WE_MIR_Z_CORR   61.5  10. V1:Sc_BS_MIR_Z_CORR  61.0   10.  #V1:Sc_PR_MIR_Z_CORR  63.0 0.
#GET_OGAIN_FREQ_BCKGRND 62 2
#GET_OGAIN 3 2 V1:Sc_NE_MIR_Z_CORR  357.5  10. V1:Sc_WE_MIR_Z_CORR  356.5  10. V1:Sc_BS_MIR_Z_CORR 356.0   10.  #V1:Sc_PR_MIR_Z_CORR 358.0 0.
#GET_OGAIN_FREQ_BCKGRND 357 2


#----------- name   coef1     channel        coef2    channel2
DEFINE_OGAIN  NE      0. V1:Sc_NE_MIR_Z_CORR_357.5  1. V1:Sc_NE_MIR_Z_CORR_62.5 51
DEFINE_OGAIN  WE      0. V1:Sc_WE_MIR_Z_CORR_356.5  1. V1:Sc_WE_MIR_Z_CORR_61.5 51

DEFINE_OGAIN  BS      0. V1:Sc_BS_MIR_Z_CORR_356.0  1. V1:Sc_BS_MIR_Z_CORR_61.0 51
DEFINE_OGAIN  PR      0. V1:Sc_PR_MIR_Z_CORR_358.0  1. V1:Sc_PR_MIR_Z_CORR_63.0 51
DEFINE_OGAIN CAVITIES 0.5 NE      0.5 WE 0

#---------faster optical gain for OMC tuning
DEFINE_OGAIN NE_11 0. V1:Sc_NE_MIR_Z_CORR_357.5  1. V1:Sc_NE_MIR_Z_CORR_62.5 11
DEFINE_OGAIN NE_21 0. V1:Sc_NE_MIR_Z_CORR_357.5  1. V1:Sc_NE_MIR_Z_CORR_62.5 21

#--------- this is to get a gain of 1
GET_OGAIN 1 2 V1:B1   62.5  0.
DEFINE_OGAIN  ONE     0. V1:B1_62.5  1. V1:B1_62.5

##-------------------------------------------------------Finesse
FINESSE_ADJUST 430 455 NE 0.5 V1:Sc_NE_MIR_Z_CORR_62.5 WE 0.5 V1:Sc_WE_MIR_Z_CORR_61.5 BS 0. V1:Sc_BS_MIR_Z_CORR_61.0 21

##-------------------------------------------------------Define the output channels
H_FREQUENCY 20000 HREC_PREFIX_hoft_20000Hz
H_FREQUENCY 16384 HREC_PREFIX_hoft_16384Hz
H_FREQUENCY 200   HREC_PREFIX_hoft_2_200Hz 1 2

#-------------------------
RANGE_CHANNEL HREC_PREFIX_hoft_20000Hz

#----------------------------------------
SAVE_FFT V1:B1 0. 2000. 500
SAVE_FFT V1:Sc_BS_MIR_Z_CORR 0. 2000. 500
SAVE_FFT V1:Sc_PR_MIR_Z_CORR 0. 2000. 500
SAVE_FFT V1:Sc_NE_MIR_Z_CORR 0. 2000. 500
SAVE_FFT V1:Sc_WE_MIR_Z_CORR 0. 2000. 500
SAVE_FFT V1:Sc_NE_MAR_Z_CORR 0. 2000. 500
SAVE_FFT V1:Sc_WE_MAR_Z_CORR 0. 2000. 500
SAVE_FFT V1:Sc_BS_MAR_Z_CORR 0. 2000. 500
SAVE_FFT HREC_PREFIX_hoft_Watt   0. 2000. 500
```

B.2 Description of main input channels: HRec_MainChannels_FromPCal.cfg

```
#-------Channels used for the reconstruction of hoft_raw; the first channel must be B1
#        name     Gain (W)       delay    debug    OpticalGainName
B1_AA_FILTER 10000. 8 #8th order Butterworth filter of B1 sensing
CHANNEL   V1:B1   -1.e-3        -58.e-6    0       CAVITIES  0. NONE
# remark: -12 ?s from 1 MHz/IRIG-B ; +152 ?s from 20 kHz/1 MHz ; -82 ?s that is the delay of the AA correction used in HRec
# and a sign "-"

#                          Gain is in m/V, delay in s

# include 10 ?s which is the extra-delay of NE,WE optical response wrt to GW optical response
CHANNEL   V1:Sc_NE_MIR_Z_CORR    0.4833e-6  -172.2e-6    0  NE 0. NONE
ADD_POLE    0.6    1000
ADD_POLE   123.46     0
ADD_ZERO   129.81     0

CHANNEL   V1:Sc_WE_MIR_Z_CORR    0.4007e-6  -171.2e-6     0 WE  0. NONE
ADD_POLE    0.6   1000
ADD_POLE   113.04     0
ADD_ZERO   115.22     0


CHANNEL   V1:Sc_BS_MIR_Z_CORR    1.07025e-6  +383.6e-6    0 BS  0.  NONE
ADD_POLE    0.6   1000
ADD_ZERO    649.3    0.6602
ADD_ZERO   1225.3    1.6026

CHANNEL   V1:Sc_PR_MIR_Z_CORR    0.8253e-6   -179.0e-6    0 PR 0. NONE
ADD_POLE    0.6   1000
ADD_POLE  304.9      0
# Optical response: only the cavity pole.

CHANNEL   V1:Sc_NE_MAR_Z_CORR    1.3529e-6   +749.4e-6    0 NE 0. NONE
ADD_POLE    0.6   1000
ADD_POLE    0.6   1000
ADD_POLE   62.77     0
ADD_ZERO   100.19     0

CHANNEL   V1:Sc_WE_MAR_Z_CORR    1.3581e-6   +701.4e-6    0 WE 0. NONE
ADD_POLE    0.6   1000
ADD_POLE    0.6   1000
ADD_POLE   60.25     0
ADD_ZERO   92.56     0

CHANNEL   V1:Sc_BS_MAR_Z_CORR   -4.7865e-6  +1043.0e-6    0 BS 0. NONE
ADD_POLE    0.6   1000
ADD_POLE    0.6   1000
ADD_POLE    51.69    0.
ADD_ZERO    83.37    0.
```

B.3 Description of hardware injection channels: HRec_CalChannels_fromPCal

```
#--------------Remove external noise used to check h_raw uncertainties

# include 10 ?s which is the extra-delay of NE,WE optical response wrt to GW optical response
# same response as for Sc_NE_MIR_Z_CORR (DeltaL/Sc) multiplied by Sc/CAL response
CHANNEL   V1:CAL_NE_MIR_Z_NOISE    0.4829e-6  +240.3e-6    0  NE 0. NONE
ADD_POLE    0.6    1000
ADD_POLE   123.46     0
ADD_ZERO   129.81     0
ADD_POLE   8174.0     0
ADD_POLE   8174.0     0

CHANNEL   V1:CAL_WE_MIR_Z_NOISE    0.4008e-6  +241.3e-6     0  WE  0. NONE
ADD_POLE    0.6   1000
ADD_POLE   113.04     0
ADD_ZERO   115.22     0
ADD_POLE   8174.0     0
ADD_POLE   8174.0     0

#--------------Remove PCal permanent lines
# PCAL delay is 112 ?s for PD1 sensing, the end mirror optical response is 10 ?s: -112 + 10 ?s = -102 ?s
# hpcal channels are in h, gain is needed to convert them into meters

CHANNEL   V1:PCAL_NEB_PD2_hpcal    -3000.  -102e-6    0  NE 0. NONE

CHANNEL   V1:PCAL_WEB_PD2_hpcal    -3000.  -102e-6    0  WE 0. NONE


#--------------Remove Hardware injections
```

B.4 Description of noise subtraction channels: HRec_NoiseChannels.cfg

```
# Reconstruction channels to get hoft_clean
CHANNEL   V1:SPRB_B4_56MHz_Q  1e-20        0.    0       ONE  0. NONE
ADD_DTF   8 90 500 40 5 .04 18
ADD_DTF_HOLE  50    1.0 2
#ADD_DTF_HOLE  50 1. 2
SAVE_FFT V1:SPRB_B4_56MHz_Q 0. 3000. 1000

#--------------Define the raw channel after frequency noise subtraction  (temporary channel for checks)
H_FREQUENCY 20000 HREC_PREFIX_hoft_clean_B4_20000Hz

#--------------Remove frequency noise
CHANNEL   V1:SIB2_B2_8MHz_I  1e-20        0.    0       ONE  0. NONE
ADD_DTF   90 3500 500 40 5 .04 18 # /users/mours/Hrec/V1O2Repro2A/tuneB2cor/InitAug1.gwf
ADD_DTF_HOLE  50    1.0 2
ADD_DTF_HOLE  730.3 1.0 0
#ADD_DTF_HOLE  50 1. 2
SAVE_FFT V1:SIB2_B2_8MHz_I 0. 3000. 1000

#--------------Define the raw channel after frequency noise subtraction  (temporary channel for checks)
H_FREQUENCY 20000 HREC_PREFIX_hoft_clean_B4_B2_20000Hz


#--------------Remove 56MHz RIN noise
CHANNEL   V1:SDB2_B1s1_PD1_Blended  1e-20        0.    0       ONE  0. NONE
ADD_DTF   40 1000 500 40 5 .04 18
ADD_DTF_HOLE  50 1. 12
ADD_DTF_HOLE  448 20. 2
ADD_DTF_HOLE  19.1 0.2 0
ADD_DTF_HOLE  67.1 0.2 0
ADD_DTF_HOLE  63.0 1.0 0
SAVE_FFT V1:SDB2_B1s1_PD1_Blended 0. 2000. 1000

#--------------Remove B7 scattered light
CHANNEL   V1:SNEB_B7_DC  1e-20        0.    0       ONE  0. NONE
ADD_DTF   10 70 500 40 5 .04 18
ADD_DTF_HOLE  5 0.1 14
ADD_DTF_HOLE  50 1. 2
ADD_DTF_HOLE  55 0.3 0
ADD_DTF_HOLE  19.1 0.2 0
ADD_DTF_HOLE  67.1 0.2 0
ADD_DTF_HOLE  63.0 1.0 0
SAVE_FFT V1:SNEB_B7_DC     0. 2000. 1000

#--------------Remove B8 scattered light
CHANNEL   V1:SWEB_B8_DC  1e-20        0.    0       ONE  0. NONE
ADD_DTF   10 70 500 40 5 .04 18
ADD_DTF_HOLE  5 0.1 14
ADD_DTF_HOLE  50 1. 2
ADD_DTF_HOLE  55 0.3 0
ADD_DTF_HOLE  19.1 0.2 0
ADD_DTF_HOLE  67.1 0.2 0
ADD_DTF_HOLE  63.0 1.0 0
SAVE_FFT V1:SWEB_B8_DC     0. 2000. 1000
```

C Other online HRec configurations

The same application version is being run online during O3, but with three other configurations useful for tests and detector monitoring:

- HRecPD1: same configuration as HRec, but using only B1_PD1 photodiode instead of the sum of B1_PD1 and B1_PD2.
- HRecPD2: same configuration as HRec, but using only B1_PD2 photodiode instead of the sum of B1_PD1 and B1_PD2.
- HRecClean: same configuration as HRec, but with some additional channels that can be subtracted to test noise subtraction.